

VALIDATION AND INTERCOMPARISON OF A 'BOTTOM-UP' AND 'TOP-DOWN' MODELING PARADIGM FOR ESTIMATING CARBON AND LATENT HEAT FLUXES OVER A VARIETY OF VEGETATIVE REGIMES ACROSS THE U.S.

7.2

Rasmus Houborg* and Martha C. Anderson
USDA-ARS Hydrology and Remote Sensing Laboratory, Beltsville, MD

1. Introduction

An accurate quantification of energy and carbon fluxes is of great importance for a wide range of ecological, agricultural, and meteorological applications. To name a few, the modeling of atmosphere-land exchange processes at a range of spatial and temporal scales can improve our understanding of ecosystem functioning, is important in the context of climate change for the establishment of regional and global carbon budgets, and have utility in water resource management and a variety of forecasting applications such as yield forecasting and numerical weather prediction.

Plant physiological research carried out in the 1980s and early 1990s provided new insights into the biochemical mechanisms controlling CO₂ assimilation of leaves and how stomata responds to environmental and physiological factors (e.g. Farquhar et al., 1980; Ball et al., 1987; Collatz et al., 1991). Stomata simultaneously regulate the conflicting demands of allowing CO₂ assimilation by leaves and minimizing the water loss from the leaves to the environment, and stomatal conductance has been recognized as a key for assessing carbon and latent heat exchange between vegetated surfaces and the atmosphere. The predictive power of biophysical models has been significantly enhanced by coupling fluxes of carbon dioxide and water vapor using semi-empirical models of stomatal functioning (e.g. Wang & Leuning, 1998; Anderson et al., 2000; Kellomäki and Wang, 2000; Sellers et al., 1996; Zhan & Kustas, 2001; Baldocchi & Wilson, 2001; Anderson et al., 2008).

Biophysical models intended for routine applications at larger scales should be capable of realistically simulating the response of canopy-scale CO₂ and energy fluxes to environmental and physiological forcings but should also remain computationally inexpensive and be sufficiently simple to be effectively parameterized over larger scales.

Two contrasting modeling strategies are currently used widely to quantify canopy-scale exchange processes of carbon and water vapor at local, regional and global scales. 'Bottom-up' models of land-atmosphere carbon and energy exchange are based on detailed mechanistic descriptions of leaf-level photosynthetic processes scaled to the canopy whereas

'top-down' scaling approaches neglect the behavior of individual leaves and consider the canopy response to its environment in bulk. 'Bottom-up' models of coupled carbon-water vapor exchange rely on the specification of an appropriate leaf-to-canopy scaling framework. Big-leaf models, that treat the canopy as a single leaf have been used extensively in land-surface parameterizations for use in climate models (e.g. Sellers et al., 1996; Dickinson et al., 1998) but have been shown to overestimate canopy photosynthesis by up to 50% at some instants (De Pury & Farquhar, 1997). Multi-layer integration schemes (e.g. Leuning et al., 1995; Baldocchi et al., 2002) consider multiple layers with many different leaf angle classes and numerically integrate fluxes for each leaf class and layer to derive total canopy fluxes. The complexity and high computational demand is an evident drawback of the multi-layer approach. The two-leaf concept represents a simplified canopy integration scheme that largely overcomes the limitations of 'big-leaf' models as it considers the highly non-linear response of leaf photosynthesis to the level of irradiance and distinctly different light environments of sunlit and shaded leaves (De Pury & Farquhar, 1997; Wang & Leuning, 1998). 'Bottom-up' (scaled-leaf) models generally require the specification of many species-dependent leaf-scale parameters but have proven effective in reproducing observed fluxes at a range of scales (Leuning et al., 1998; Houborg & Soegaard, 2004; Zhan & Kustas, 2001; Dai et al., 2004).

'Top-down' models are generally less complex as they are constrained by some empirical relationship developed at the stand level and thus implicitly incorporate scaling effects. The light-use-efficiency (LUE), defined as the ratio between net CO₂ assimilation rate and absorbed photosynthetically active radiation (APAR) is a fundamental quantity used by a suite of simple biophysical models (e.g. Ruimy et al., 1994; Prince & Goward, 1995) that assume conservation of LUE within major vegetation groups when plants are unstressed. Models constrained by LUE generally require the specification of only few tunable parameters.

The objective of this study is to compare a simple analytical light-use efficiency (LUE)-based model of canopy resistance with a mechanistic model of leaf-level photosynthesis – stomatal response that employs a 'two-leaf' scaling strategy. For the purpose of inter-comparisons both canopy sub-models have been embedded in the Atmosphere-Land Exchange (ALEX) surface energy balance model, which is a

* Corresponding author address: Rasmus Houborg, USDA-ARS Hydrology and Remote Sensing Lab, 10300 Baltimore Ave, Beltsville, MD, e-mail: Rasmus.houborg@ars.usda.gov

simplified version of a detailed soil-plant-atmosphere model Cupid, specifically developed for operational applications. The ability of the two canopy sub-models to reproduce observed patterns in energy and carbon fluxes across time scales of hours, days, seasons and years is effectively evaluated for a variety of natural and agricultural ecosystems. Comparisons are done using several years of field data compiled from AmeriFlux sites across the U.S.

2. CANOPY-SCALE MODEL OF ATMOSPHERE LAND EXCHANGE (ALEX)

At the core of the prognostic canopy-scale model of atmosphere-land exchange (ALEX) is a two-layer (soil and vegetation) land surface representation coupling conditions inside the canopy to fluxes from the soil, plants, and atmosphere. The ALEX model is described in detail in Anderson et al. (2000) and is only briefly summarized here. The conceptual structure of the ALEX model is given in Fig. 1 where the directions of fluxes are those typical for daytime conditions. The latent heat flux at the measurement reference height (LE) represents water vapor evaporation from the insides of leaf stomates (LE_c) and the soil surface (LE_s), H is sensible heat transferred from the canopy air space (the subscript 'ac' designates conditions within the canopy air space) due to sensible heat convection or conduction from leaf (H_c) and soil surface (H_s), and A is the net ecosystem CO_2 exchange which incorporates the assimilation of CO_2 inside plant leaves through the stomates (A_c) and respiratory loss of CO_2 from soil and roots (A_s) and from leaf foliage. In ALEX these fluxes are regulated by series-parallel resistance networks that allow both soil and canopy components of the system to modify the in-canopy air temperature and vapor pressure.

For the purpose of this study two alternative sub-models for estimating canopy fluxes of water and carbon were embedded in ALEX. The two sub-models share the ALEX two-layer land surface representation (Fig. 1) but differ distinctly in the way the photosynthesis-stomatal response is described. The 'bottom-up' (scaled-leaf) canopy sub-model is constructed from mechanistic representations of leaf-level photosynthetic processes scaled to the canopy level, whereas the 'top-down' scaling approach of the light-use-efficiency (LUE)-based sub-model considers the canopy response to its environment in bulk, neglecting the behavior of individual leaves. In both canopy sub-models, stomatal closure in response to water stress is simulated through incorporation of an

empirical stress function (Norman, 1979; Campbell & Norman, 1998) that relates depletion of the fraction of plant available water in the root zone to reductions in transpiration/assimilation due to stomatal closure.

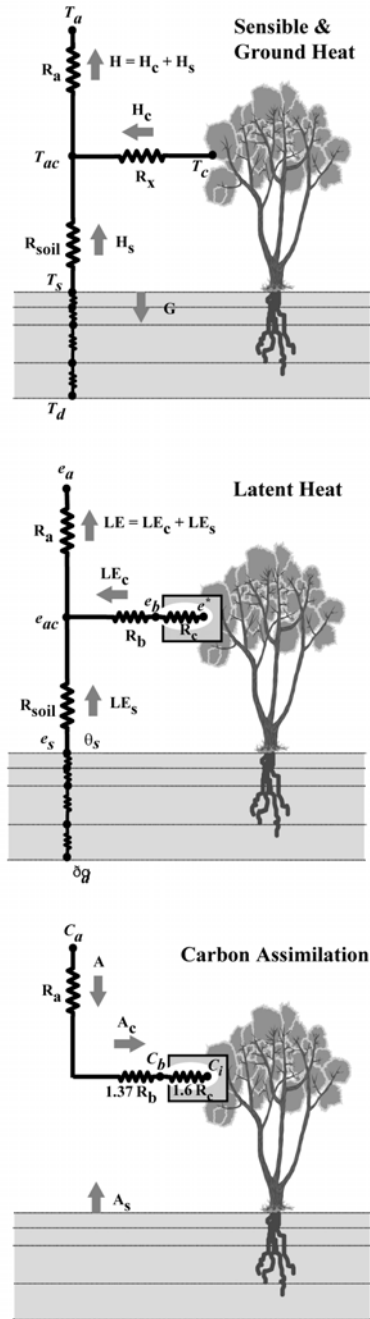


Fig. 1. Transport resistance networks used in the ALEX model to estimate fluxes of (a) sensible and soil heating, (b) latent heating and (c) assimilated carbon. The subscripts 'a', 'ac', 'b', and 'i' refer, respectively, to conditions above the canopy, within the canopy air space, within the boundary layer at the leaf surface, and inside sub-stomatal cavities. The 1.6 and 1.37 resistance multipliers account for the difference in diffusivity between CO_2 and water vapor.

The two canopy sub-models are detailed in the next two sections.

In ALEX, the soil heat flux (G) and soil evaporation rate is predicted by a multi-layered numerical soil model that serves as the lower boundary to ALEX. This soil transport module is a generalization of algorithms from Campbell (1985), adapted to a soil structure with layered hydraulic and thermal properties. Profiles of soil temperature (T_s) and water content with depth are updated by solving systems of second-order, time-dependent differential equations using a Newton-Raphson finite-difference solution technique.

2.1. Scaled-leaf canopy sub-model ('bottom-up')

In the scaled-leaf model, canopy photosynthesis is modeled by applying mechanistic equations of photosynthesis-stomatal response defined at the leaf scale, and by separating leaves into sunlit and shaded fractions to facilitate scaling from leaf to canopy. The model employs the biochemical equations of leaf photosynthesis by Farquhar, Collatz and collaborators (Farquhar et al., 1980; Collatz et al., 1991; Collatz et al., 1992), and couples CO_2 assimilation and stomatal conductance using a semi-empirical model of stomatal functioning (Ball et al., 1987). The equations of the coupled CO_2 assimilation, stomatal conductance and latent heat flux models are summarized in Table 1A.

Within this integrated model, leaf-level photosynthesis for C_3 and C_4 photosynthetic pathways is estimated as the minimum of the Rubisco-limited rate of ribulose biphosphate (RuBP) carboxylation (Eq. A2), the electron transport limited (light-limited) rate of RuBP regeneration (Eq. A3), and the Carbon compound export limited (C_3) or PEP-carboxylase limited (C_4) rate (Eq. A4) minus dark respiration, i.e. leaf respiration (R_d). The rate of CO_2 assimilation for C_3 and C_4 plants is solved from nested quadratics (Eq. A6) to allow for a gradual transition and co-limitation between the three capacities.

The strong non-linear variation of photosynthetic model parameters with temperature is described by an Arrhenius function (Eq. A10). A de-activation function (Eq. A11) was incorporated in the temperature response functions for the maximum Rubisco capacity (V_m) and the Potential rate of electron transport (J_m) to simulate a drop in activity at extreme temperatures. V_m and J_m was reduced from their potential values when soil water is limiting by multiplication with the fraction of available water (f_{aw}) as photosynthetic capacity has been shown to decrease in response to soil water deficits (Wilson et al., 2001). The system of equations describing leaf photosynthesis and stomatal conductance (Eq. A1 – A10) are solved separately for C_3 and C_4 vegetation using cubic analytical solutions (Baldocchi, 1994; Collatz et al., 1992) to avoid the tendency of iterative solutions techniques to arrive at chaotic solutions under spe-

cific extreme conditions (Baldocchi, 1994). The resultant stomatal conductance is then used as input to the latent heat flux equation (Eq. A11).

Total canopy photosynthesis and transpiration are calculated as the sum of contributions from sunlit and shaded canopy fractions. This 'two-leaf' scaling strategy is generally assumed more reliable than 'big-leaf' models that treat the canopy as a single leaf, due to the highly non-linear response of leaf photosynthesis to the level of irradiance and distinctly different light environments of sunlit and shaded leaves (De Pury & Farquhar, 1997; Wang & Leuning, 1998). The leaf to canopy scaling principles adopted here assume that 1) the maximum Rubisco capacity is linearly related to leaf nitrogen and that nitrogen allocation decline exponentially from the top of the canopy (De Pury & Farquhar, Wang & Leuning, 1998), and 2) the vertical profile of the potential rate of electron transport parallels that of light (Wang & Leuning, 1998). The leaf to canopy scaling equations were modified to consider the clumping effect (Eq. A13 – A17). The partitioning of absorbed photosynthetically active radiation (APAR) into sunlit and shaded canopy fractions is done according to De Pury & Farquhar (1997) by considering direct-beam, diffuse and scattered beam irradiance. The partitioning of the canopy net-radiation into sunlit and shaded canopy fractions follows Zhan & Kustas (2001).

2.2. LUE-based sub-model ('top-down')

The equations describing the light-use-efficiency (LUE)-based sub-model are given in Anderson et al. (2000) and summarized in Table 1B to facilitate a direct comparison with the 'scaled-leaf' sub-model. Nominal stand-level measurements of LUE (β_n) and nominal estimates of the ratio of intercellular to ambient CO_2 concentration (γ_n) replace the mechanistic leaf-level photosynthetic equations (Eq. A1 – A8). Since CO_2 assimilation scaling effects are implicitly incorporated into the measurement of β_n , the leaf to canopy scaling equations (Eq. A14 – A18) are also avoided. This modeling paradigm exploits the conservative quality of canopy LUE that is observed over a seasonal to annual timescales within broad vegetation categories under unstressed environmental condition. Deviations of the canopy LUE from this nominal value on shorter timescales is accommodated by diagnosing an effective LUE (β) that responds linearly to changes in the ratio of intercellular to ambient CO_2 concentration ($\gamma=C_i/C_a$) (Eq. B7) and the fraction of diffuse radiation (Eq. B8). The model paradigm assumes that under optimal conditions the canopy will tend to operate near β_n with a nominal value of γ (γ_n). An increase in the stomatal resistance in response to e.g. a desiccating environment will decrease the average C_i and move the canopy toward a lower value of LUE. CO_2 assimilation is linked to canopy stomatal conductance using the approach of Ball et al. (1987) (Eq. B4) and the canopy stomatal

Table 1. List of flux tower sites, vegetation and soil types and climatic conditions

Site	ID	Latitude Longitude	Study period	Landcover class	Soil type	Precip [mm]	Mean T_a [°C]
Audubon Ranch	AG	31° 35 27 N 110° 30 37 W	Jan – Dec (2003 – 2006)	Grassland	Sandy loam	356	15.9
Fort Peck	FP	48° 18 28 N 105° 06 02 W	May – Sept (2003 – 2006)	Grassland	Clay loam	218	17.0
Goodwin Creek	GC	34° 15 00 N 89° 58 12 W	April – Oct (2003 – 2006)	Grassland	Silt loam	636	22.3
Bondville	BV	40° 00 22 N 88° 17 24 W	May – Sept (2003 – 2006)	Cropland	Silt loam	415	20.6
Bondville companion	BP	40° 00 33 N 88° 17 26 W	May – Sept (2004 – 2005)	Cropland	Silt loam	415	21.1
Black Hills	BH	44° 09 29 N 103° 39 00 W	May – Oct (2003 – 2006)	Evergreen needleleaf	Clay loam	388	13.2
Walker Branch	WB	35° 57 32 N 84° 17 15 W	April – Oct (2003 – 2006)	Deciduous broadleaf	Silty clay loam	708	18.6

resistance is derived using a second-order analytical expression (see Eq. 11 in Anderson et al., 2000) semi-constrained by β_n and γ_n averaged over broad vegetation categories. The modeled canopy stomatal resistance responds to changes in soil moisture availability and varying environmental conditions in humidity, temperature (ambient and leaf), wind speed, CO₂ concentration, and direct beam vs. diffuse light composition. The fraction of available water (faw) is multiplied with the stomatal slope factor (m) as experimental evidence suggests decreasing m as soil water deficits develop.

3. FLUX TOWER DATASETS

Eddy-covariance based measurements of surface heat, water and carbon dioxide fluxes were obtained from 7 NOAA GEWEX (Global Energy and Water Cycle Experiment) air SURFace eXchange (SURFX) sites (<http://www.atdd.noaa.gov/gewex.htm>) representing diverse land vegetation environments (Table 1). These sites are also included in the AmeriFlux network (<http://public.ornl.gov/ameriflux/>) and the measurements and instrumentation follow the AmeriFlux protocol (Baldocchi, 2003). Net ecosystem CO₂ exchange is the sum of the CO₂ flux densities measured by the eddy covariance systems and a CO₂ storage term that accounts for CO₂ stored in the layer of air below the eddy covariance system. This storage may be significant for forest ecosystems especially at night when the atmosphere is stable and winds are weak (Wofsy et al., 1993). CO₂ flux densities not corrected for storage may show spikes in CO₂ assimilation shortly after sunrise when convective turbulence resumes and CO₂ is vented from the canopy into the turbulent boundary layer. The CO₂ flux densities presented in this paper have not been corrected for storage but are assumed representative of the net rate of ecosystem exchange. Carbon gained by the ecosystem is treated as a positive flux. All other flux densities (mass and energy fluxes) are defined as positive away from the surface. Strict acceptance/reject criteria were applied to the flux meas-

urements and the flux records used to validate the models were not gap-filled.

A correction was applied to the soil heat flux data measured at a depth of 2 cm to account for heat storage that occurs in the layer between the soil surface and the heat flux plate. The corrections were done as described in Mayocchi & Bristow (1995) and consider the time rate of change in soil temperature above the plate and the volumetric heat capacity that varies as a function of soil bulk density, soil texture, organic matter content and soil water content.

Sensible and latent heat fluxes measured by eddy covariance are typically less than the difference between net radiation and soil heat fluxes, and this lack of closure of the surface energy balance has been shown to be on the order of 10 – 30 % of measured net radiation (e.g. Twine et al., 2000; Anderson et al., 2000). In this study, closure among energy flux components was enforced by modifying the observed sensible and latent heat fluxes such that they summed to the available energy yet retained the observed Bowen ratio, as this has been found to be the preferred method of energy balance closure (Twine et al., 2000).

Ancillary observations of incoming solar radiation, longwave incoming radiation, relative humidity, air temperature, atmospheric pressure, precipitation and leaf area index were used as input to the ALEX model. At each site, seasonally distributed LAI data are being deduced as an exponential function of NDVI estimated continuously using 30-min solar radiation and photosynthetically active radiation data (Wilson & Meyers, 2007).

Descriptive landcover classes were assigned to each flux tower site based on the University of Maryland (UMD) 1-km global landcover product (Hansen et al., 2000). Site details are given below and in Table 1.

3.1. Grasslands

Measurements from three climatologically distinct grassland sites were used (Table 1). The Audu-

bon Research Ranch (AG) is a non-grazed desert grassland site located in the plateaus of southwestern Arizona. The tower is located at an elevation of approximately 985 m and is surrounded with scattered short grasses and shrubs. The major dominant C₃ shrub is creosote bush (*Larrea tridentate*) and grasses are dominated by *Bouteloua* species (C₄). Mean air temperatures during the study period (2003 – 2006) ranged from a January minimum of 2 °C to a June maximum of 33 °C, and average annual rainfall was 365 mm most of which occurred during the summer (July to September) monsoon season. The area is dominated by soils of the White horse series (gravelly/sandy loam) with a significant fraction of rocks (~35 %).

Fort Peck (FP) is a northern plain grassland site in northeastern Montana. The tower is located approximately 634 m above sea level and is characterized by a mixture of perennial grasses with C₃ (e.g. *Agropyron dasystachyrum* (Hook.) Scrib and *Pascopyron smithii* Rydb) and C₄ (e.g. *Bouteloua gracilis* (H.B.K.) Lag) photosynthetic pathways (Gilmanov et al., 2005). The average precipitation during the growing season that normally runs from May to September was 218 mm (2003 – 2006). The soil has been classified as clay loam.

The Goodwin Creek (GC) experimental watershed is located in northwestern Mississippi and is characterized as temperate wetted grassland. The average precipitation during the April to October study period (2003 – 2006) totaled 636 mm and the average air temperature was 22 °C (Table 1). The flux tower is situated at an elevation of 105 m on well-drained soils with silt loam textures and is surrounded by a mixture of C₃ short grasses (e.g. *Panicum virgatum* L. - switch grass), C₄ grasses (e.g. *Bouteloua gracilis* (H.B.K.) Lag), scattered trees and shrubs (*salix spp.*). It is a grazed site where the growing season typically runs from March to October.

3.2. Cropland

Data from cropland were acquired from two adjoining flux tower sites, separated by a north-south distance of ~ 400 m, located on a farm south of Champaign in eastern Illinois. The south tower, denoted as BV, has been under no-till management since 1986 whereas the north tower, denoted as BP, began operation in late 2003. Crop production rotates yearly between corn (*Zea mays*, C₄) and soybean (*Glycine max*, C₃). The soils are silt loam. The fields surrounding these stations received around 415 mm of precipitation on average during the 2003 – 2006 growing seasons (Table 1).

3.3. Evergreen needle-leaf forest

Model validations and intercomparisons were also performed using measurements acquired during the freeze-free season (May – October) at the Black

Hills (BH) experimental forest site located in western South Dakota 1715 m above sea level. The flux tower was established in 2001 by the Institute for Atmospheric Studies of the South Dakota School of Mines and Technology (SDSM&T). The vegetation around the tower is dominated by ~17 m tall Ponderosa Pine (*Pinus ponderosa*) (99 %) and the forest floor is completely covered with a thick (~ 10 cm) layer of dead plant materials. The soil has been classified as clay loam. The climate is temperate and the site received an average precipitation total of 388 mm during the period of interest for this study (Table 1).

3.4. Deciduous broadleaf forest

The Walker Branch (WB) flux tower is located on the United States Department of Energy reservation near Oak Ridge in the ridge and valley province of eastern Tennessee. The site is 335 m above sea level and is classified as an Eastern, mixed-species, broad-leaved deciduous forest. Oak (*Quercus alba* L., *Q. prinus* L.), hickory (*Carya ovata* (Mill.) K. Koch), maple (*Acer rubrum* L., *A. saccharum*), tulip poplar (*Liriodendrom tulipifera* L.), black gum (*Nyssa sylvatica* Marsh) and loblolly pine (*Pinus taeda* L.) dominate the forest canopy surrounding the flux tower (Baldocchi & Wilson, 2001). Leaf emergence typically occurs between day of year (doy) 90 and 110 and autumnal senescence begins around doyr 280. The average rainfall during this period for the years 2003 – 2006 was 708 mm. The predominant soils are classified as silty-clay loam and the forest floor is covered by a ~10 cm thick residue layer throughout the year. Hourly measurements of soil surface CO₂ fluxes, used for validating the applied soil respiration model (section 4.5), were obtained from chamber measurements at the base of the Chestnut Ridge flux tower located 5 km south west of the Walker Branch Flux tower. The chamber is attached to a LI-COR LI-6400 gas analyzer system and has been operating continuously since 2006.

4. MODEL SETUP

A complete list of soil, leaf and canopy parameter values used in the ALEX simulations are given in Table 2. The parameters are listed for each of the vegetation environments associated with the flux tower sites and were determined based on generalized data reported in the ecological literature. The parameterizations are intended to be representative for broad categories of vegetation environments as ALEX and its associated applications (see Anderson et al., 2003 for an overview) are intended for regional to continental-scale flux modeling.

4.1. Shared model parameters

Table 2. A complete list of soil, leaf and canopy parameter values used in the ALEX simulations

Parameter	ID	Units	AG	FP	GC	BV	BP	BH	WB
<i>Shared canopy parameters</i>									
Ambient CO ₂ concentration	C_a	$\mu\text{mol mol}^{-1}$	360	360	360	360	360	360	360
Leaf area index	L	m m^{-1}	0.2 – 1.1	0.1 – 4.7	0.1 – 3.8	0.1 – 5.1	0.1 – 6.1	0.5 – 4.2	0.5 – 7.5
Fraction of green vegetation	f_g		1.0	1.0	1.0	0.1 – 1.0	0.1 – 1.0	1.0	0.1 – 1.0
Canopy height	h_c	m	0.2	0.1 - 0.4	0.1 - 0.4	0 – 3.0	0 – 0.9	24	25
Clumping factor at nadir	Ω		0.7	1.0	1.0	0.9	1.0	0.5	0.90
Ratio of canopy width to height	D		1.0	1.0	1.0	1.0	1.0	3.5	1.0
Surface roughness	Z_m	m	$0.16h_c$	$0.05h_c$	$0.05h_c$	$0.1h_c$	$0.1h_c$	$0.1h_c$	$0.1h_c$
Displacement height	d	m	$0.44h_c$	$0.67h_c$	$0.67h_c$	$0.67h_c$	$0.67h_c$	$0.67h_c$	$0.67h_c$
Average leaf size	s	m	0.02	0.02	0.02	0.2	0.03	0.05	0.10
Ball & Berry slope	m		11.0	9.5	9.5	3.5	9.5	9.5	9.5
Ball & Berry offset	b	$\mu\text{mol m}^{-2} \text{s}^{-1}$	0.01×10^6	0.01×10^6	0.01×10^6	0.04×10^6	0.01×10^6	0.01×10^6	0.01×10^6
Minimum RH in Ball & Berry	$RH_{b,mi}$		0.6	0.1	0.1	0.1	0.1	0.1	0.1
Stomatal distribution correction factor ¹	f_c		2	2	2	2	2	2	1
Fraction of plants with C ₃ pathway	f_{c3}		0.6	0.9	0.6	0.0	1.0	1.0	1.0
Leaf absorptivity (vis) (live)	a_{lv}		0.82	0.82	0.82	0.83	0.83	0.89	0.86
Leaf absorptivity (nir) (live)	a_{ln}		0.28	0.28	0.28	0.35	0.35	0.6	0.37
Leaf absorptivity (vis) (dead)	a_{dv}		0.42	0.42	0.42	0.49	0.49	0.84	0.84
Leaf absorptivity (nir) (dead)	a_{dn}		0.04	0.04	0.04	0.13	0.13	0.61	0.61
Rooting depth	d_r	m	2.0	2.0	2.0	2.0	2.0	2.0	2.0
Max interception	$W_{i,max}$	mm	0.15	0.15	0.15	0.15	0.15	0.15	0.15
Max fraction of wetted leaf area	$f_{wet,max}$		0.2	0.2	0.2	0.2	0.2	0.2	0.2
<i>LUE module</i>									
Nominal LUE	β_n	mol mol^{-1}	0.02/0.03	0.013/0.03	0.013/0.03	0.040	0.024	0.014	0.022
Nominal C_i/C_a fraction	γ_n	mol mol^{-1}	0.7/0.5	0.7/0.5	0.7/0.5	0.5	0.7	0.7	0.7
C_i/C_a at $\beta=0$	γ_0	mol mol^{-1}	0.2/0.0	0.2/0.0	0.2/0.0	0.0	0.2	0.2	0.2
<i>Scaled-leaf module</i>									
Maximum Rubisco capacity	V_m^{25}	$\mu\text{mol m}^{-2} \text{s}^{-1}$	122/20	63/20	63/20	30	95	42	53
Leaf respiration	R_d^{25}	$\mu\text{mol m}^{-2} \text{s}^{-1}$	$0.015V_m^{25}$	$0.015V_m^{25}$	$0.015V_m^{25}$	$0.025V_m^{25}$	$0.015V_m^{25}$	$0.015V_m^{25}$	$0.015V_m^{25}$
Nitrogen extinction coefficient	k_n		0.7	0.7	0.7	0.7	0.7	0.5	0.5
Quantum yield for electron transport	α_3	mol mol^{-1}	0.37	0.37	0.37		0.37	0.37	0.37
C4 quantum yield for CO ₂ uptake	α_4	mol mol^{-1}	0.062			0.062			
Initial slope of photosynthetic CO ₂	k	$\text{mol m}^{-2} \text{s}^{-1}$	$20 \times 10^3 V_m^{25}$			$20 \times 10^3 V_m^{25}$			
Potential rate of electron transport	J_m^{25}	$\mu\text{mol m}^{-2} \text{s}^{-1}$	$1.9V_m^{25}$	$1.9V_m^{25}$	$1.9V_m^{25}$	$1.9V_m^{25}$	$1.9V_m^{25}$	$1.9V_m^{25}$	$1.9V_m^{25}$
Curvature factor	θ_j		0.7	0.7	0.7	0.7	0.7	0.7	0.7
Oxygen partial pressure	O	mmol mol^{-1}	205	205	205	205	205	205	205
Michaelis-Menten constant for CO ₂	K_c^{25}	$\mu\text{mol mol}^{-1}$	404.9	404.9	404.9	404.9	404.9	404.9	404.9
Michaelis-Menten constant for O ₂	K_o^{25}	mmol mol^{-1}	278.4	278.4	278.4	278.4	278.4	278.4	278.4
CO ₂ compensation point *	Γ^{*25}	$\mu\text{mol mol}^{-1}$	42.75	42.75	42.75	42.75	42.75	42.75	42.75
Energy of activation for K_c^{25}	$H_{a,1}$	KJ mol^{-1}	79.43	79.43	79.43	79.43	79.43	79.43	79.43
Energy of activation for K_o^{25}	$H_{a,2}$	KJ mol^{-1}	36.38	36.38	36.38	36.38	36.38	36.38	36.38
Energy of activation for Γ^{*25}	$H_{a,3}$	KJ mol^{-1}	37.83	37.83	37.83	37.83	37.83	37.83	37.83
Energy of activation for J_m^{25}	$H_{a,4}$	KJ mol^{-1}	50.00	50.00	50.00	50.00	50.00	50.00	50.00
Energy of activation for V_m^{25}	$H_{a,5}$	KJ mol^{-1}	72.00	72.00	72.00	72.00	72.00	72.00	72.00
Energy of activation for R_d^{25}	$H_{a,6}$	KJ mol^{-1}	46.39	46.39	46.39	46.39	46.39	46.39	46.39
Energy of deactivation for V_m^{25} and J_m^{25}	H_d	KJ mol^{-1}	200.0	200.0	200.0	200.0	200.0	200.0	200.0
Entropy term for V_m^{25}	ΔS_V	$\text{KJ mol}^{-1} \text{C}^{-1}$	0.6416	0.649	0.649	0.649	0.649	0.649	0.649
Entropy term for J_m^{25}	ΔS_J	$\text{KJ mol}^{-1} \text{C}^{-1}$	0.6410	0.646	0.646	0.646	0.646	0.646	0.646
C3 curvature (co-limitation) parameter	θ_3		0.92	0.92	0.92	0.92	0.92	0.92	0.92
C3 curvature (co-limitation) parameter	β_3		0.99	0.99	0.99	0.99	0.99	0.99	0.99
C4 curvature (co-limitation) parameter	θ_4		0.83	0.83	0.83	0.83	0.83	0.83	0.83
C4 curvature (co-limitation) parameter	β_4		0.93	0.93	0.93	0.93	0.93	0.93	0.93
<i>Soil transport module</i>									
Bulk density	BD	g cm^{-3}	1.4	1.32	1.4	1.4	1.4	1.32	1.26
Moisture release parameter	b_s		3.1	5.2	4.7	4.7	4.7	5.2	6.6
Air entry potential	ψ_e	J kg^{-1}	-1.5	-2.6	-2.1	-2.1	-2.1	-2.6	-3.3
Sat. hydraulic conductivity	K_s	kg s m^{-3}	7.2×10^{-4}	6.4×10^{-5}	1.9×10^{-4}	1.9×10^{-4}	1.9×10^{-4}	6.4×10^{-5}	4.2×10^{-5}
Deep soil temperature	T_d	$^{\circ} \text{C}$	20	12	21	15	15	13	15
Soil emissivity	ϵ_s		0.96	0.96	0.96	0.96	0.96	0.96	0.96
Soil reflectance (vis)	ρ_{sv}		0.11	0.11	0.11	0.11	0.11	0.08	0.08
Soil reflectance (nir)	ρ_{sn}		0.22	0.22	0.22	0.22	0.22	0.18	0.18
Surface ponding capacity	h_{max}	mm	5.0	5.0	5.0	5.0	5.0	5.0	5.0

Leaf and soil optical (absorptivities, reflectances, emissivity) properties and nominal leaf sizes were assigned according to the ALEXI Landcover classification system (Anderson et al., 2007) which is based

on the UMD 1-km Global Landcover product (Hansen et al., 2000). The morphological properties for the cropland class were modified to take into account the distinct differences between corn and soybean culti-

Table 3. Mean and standard deviations among measurements of maximum LUE for major vegetation groups. All LUE values have been converted to units of mol CO₂ mol⁻¹ from their original units of g NPP per MJ APAR as described in Anderson et al. (2000). N indicates the number of LUE estimates used to compute the average and standard deviation

Vegetation type	N	Average LUE	Standard dev in LUE	References
C ₃ cropland (soybean)	3	0.024	0.001	Gower et al. (1999)
C ₄ cropland (corn)	6	0.040	0.002	Gower et al. (1999)
Temperate evergreen needleleaf	18	0.014	0.003	Gower et al. (1999), Ruimy et al. (1994), Runyon et al. (1994)
Temperate deciduous	8	0.020	0.006	Gower et al. (1999), Ruimy et al. (1994)
Temperate grasses	3	0.013	0.003	Ruimy et al. (1994), Kim & Verma (1990)
C ₄ grasses	1	0.030	0.000	Anderson et al. (2008)
Desert shrubs	1	0.020	0.000	Gutschick (1996)

vars. Surface roughness (Z_m) and displacement height (d) were calculated as landcover dependent fractions of the canopy height (h_c) (Massman, 1997) that is scaled linearly with the fraction of vegetation cover between a seasonal minimum and maximum value (Anderson et al., 2007). Forests have been found to exhibit a clumped stature and nadir clumping index (Ω) values reported in Gower et al. (1999) and Kucharik et al. (1999) for several forest ecosystems were adopted here. The vegetation heterogeneity at the desert grassland site, characterized by a mixture of grasses and scattered shrubs, was treated by assigning a nadir clumping factor of 0.7. Ω was assumed to be 0.9 for the C₄ cropland class (Anderson et al., 2007) whereas randomly distributed leaves were assumed for C₃ cropland and the FP and GC grassland sites ($\Omega = 1.0$). The ratio between canopy height and nominal clump width, D , is required as input to model the dependence of the clumping index on zenith angle (Kucharik et al., 1999). The leaf area index (L) record from each site (section 3) represents green L . At the agricultural and deciduous forest sites, that experienced significant degrees of senescence late in the season, the fraction of green vegetation (f_g) was calculated as green L divided by the average L during the leaf maturity period.

The slope and offset of the Ball & Berry stomatal conductance model have been found to be fairly constrained parameters within C₃ and C₄ functional categories for ample soil moisture conditions (e.g. Ball et al., 1987; Leuning, 1990; Collatz et al., 1991). Values between 9 - 10 for the stomatal slope (m) are generally assumed representative for C₃ vegetation in the mid-latitudes and plants with C₄ photosynthetic physiology are typically assigned a value between 3 - 4 (Sellers et al., 1996; Collatz et al., 2002; Kosugi et al., 2003). The steeper stomatal slope ($m = 11$) that was assigned to the desert grassland site is in accor-

dance with findings reported in Zhan & Kustas (2001) and Gutschick (1996).

A parameter describing the relative distribution of leaves with C₃ and C₄ pathways (f_{c3}) was introduced to allow mixed C₃ and C₄ canopies to be simulated. This was achieved by cycling through the LUE or scaled-leaf canopy subroutine twice using canopy parameters specific to each physiological type in each run. Total canopy estimates were then derived by weighing C₃ and C₄-specific CO₂ and energy fluxes, stomatal conductances and canopy temperatures with the relative distribution of each component within the canopy.

In the soil transport module, soil hydraulic and thermal properties were derived from tabular values in Campbell & Norman (1998) based on the assigned soil texture class (Table 1). A single-layered soil structure with uniform hydraulic and thermal properties was assumed for simplicity. A 10 cm thick residual litter layer was simulated at the forested sites by adding a soil layer with hydraulic and thermal properties characteristic of organic material (Lawrence & Slater, 2008). The deep soil temperature (T_d) was estimated for each flux tower site as the average of the observed 100 cm soil temperature during the growing season. The soil moisture profile was initialized with observations made at the flux tower sites.

4.2. LUE-based canopy sub-model

The nominal LUE (β_n) is a key input to the LUE-based canopy sub-model and should represent conditions when the environment does not constrain photosynthesis (i.e. unfavorable temperatures, drought, and high vapor pressure deficits) as these limiting factors are explicitly treated by the model (section 2.2 and Table 1B). Table 3 recapitulates mean values and standard deviations of maximum LUE measurements reported in the literature for different vegetation

Table 4. Vegetation specific V_m^{25} data based on estimates compiled in various studies. N indicates the number of V_m^{25} estimates used to compute the average and standard deviation.

Vegetation classes	N	Average V_m^{25}	Standard dev in V_m^{25}	Reference
C ₃ cropland (soybean)	7	95	38	Wullschleger (1993), Kattge & Knorr (2007)
C ₄ cropland (corn)	1	30	0	Massad et al. (2007)
Temperate evergreen needle-leaf	18	49	30	Wullschleger (1993), Kattge & Knorr (2007)
Temperate deciduous	34	54	28	Wullschleger (1993), Kattge & Knorr (2007)
Temperate grasses	12	63	14	Wullschleger (1993), Kattge & Knorr (2007)
C ₄ grasses	1	20	0	Chen et al. (1994), Kubien & Sage (2004)
Desert shrubs	3	122	28	Wullschleger (1993), Kattge & Knorr (2007)

groups, converted into units of mol CO₂ (mol APAR)⁻¹ as described by Anderson et al. (2000). These LUE values are based on annual or seasonal biomass accumulation from sites and time periods where climatic factors did not constrain photosynthesis (e.g. fertilized, irrigated, cultivated, highly productive sites), and represent here the aboveground and belowground net primary productivity (i.e. CO₂ uptake less autotrophic respiration) per mole PAR photons absorbed by the vegetation. The values have been standardized as suggested by Gower et al. (1999). As it was difficult to find literature values of β_n for C₄ grassland, this vegetation group was arbitrarily assigned a value of 0.03 according to Anderson et al. (2008).

Nominal C_i/C_a (γ_n) fractions have been determined through numerical experimentation with the Cupid model (Anderson et al., 2000) and reflect the distinctly different ratio of intercellular to ambient CO₂ concentration characteristic of canopies with C₃ and C₄ photosynthetic physiology (Wong et al., 1979; Baldocchi, 1994).

4.3. Scaled-leaf canopy sub-model

The scaled-leaf module requires the setting of many adjustable parameters and it can be a considerable challenge to assign representative vegetation-specific parameter values. The maximum catalytic capacity of Rubisco at a temperature of 25°C (V_m^{25}) and the potential rate of electron transport (J_m^{25}) are critical parameters in this canopy sub-model and they have to be specified for different species as species differ to a considerable extent in their biochemical capacity to assimilate CO₂ (Wullschleger, 1993). Vegetation specific data on V_m^{25} for C₃ vegetation were derived based on estimates compiled in Wullschleger (1993) for 109 species representing several broad plant categories and in Kattge & Knorr (2007) for 36 species covering broadleaved trees and shrubs, needle-leaved coniferous trees and grasses, and on estimates in Dreyer et al. (2001) for temperature deciduous trees. The average and standard deviation of the compiled data for vegetation groups of relevance in this study are listed in Table 4. Values in Wullschleger (1993) are provided at variable leaf temperatures and were corrected to a common reference temperature of 25°C using a peaked Arrhenius temperature response function (Eq. A14). Very little information is available in the literature on the setting of V_m^{25} for C₄ grasses and C₄ crops. For corn we use a value of 30 $\mu\text{mol m}^{-2} \text{s}^{-1}$ in accordance with leaf gas exchange measurements on maize reported in Massad et al. (2007) and Crafts-Brandner & Salvucci (2002). C₄ grasses were assigned a value of 20 $\mu\text{mol m}^{-2} \text{s}^{-1}$ in accordance with Chen et al. (1994) and Kubien & Sage (2004). The electron transport rate (J_m^{25}), leaf respiration (R_d) and the initial slope of photosynthetic CO₂ response (k) are all modeled as a function of V_m^{25} assuming that they co-vary with leaf nitrogen

(e.g. Collatz et al., 1991; Collatz et al., 1992; Wullschleger, 1993). The relationship between V_m^{25} and J_m^{25} has been widely investigated and these two component processes have been shown to be tightly coupled with reported J_m^{25}/V_m^{25} ratios of e.g. 1.67 (Medlyn et al., 2002), 1.89 (Kattge & Knorr, 2007), 2.0 (Leuning, 2002) and 2.1 (Wohlfahrt et al., 1999). An arithmetic mean of these estimates was used here for all vegetation classes as the cause of the variation (e.g. species-specific differences, environmental conditions) is currently not clear. R_d is assumed to equal 0.015 times V_m^{25} for C₃ plants and 0.025 times V_m^{25} for C₄ plants (Sellers et al., 1996). The nitrogen extinction coefficient (K_n) was fixed to 0.5 for the forest classes (Kellomaki & Wang, 2000) and to 0.7 for the remaining vegetation classes (De Pury & Farquhar, 1997) to simulate a slower rate of decrease of nitrogen concentration within forest canopies.

Ehleringer & Pearcy (1983) found the quantum yield for CO₂ uptake, α' , to be similar for a wide range of monocot and dicot C₃ species with a representative average value of approximately 0.06 at a reference temperature of 25 °C. α' was converted into the quantum yield of electron transport (α_3) following von Caemmerer & Farquhar (1981), using $\alpha=4\alpha'/(C_i+2\Gamma^*)/(C_i-\Gamma^*)$ and fixing C_i to 280 $\mu\text{mol mol}^{-1}$. The resultant quantum yield ($\alpha_3 = 0.367$) was adopted for all simulations (Table 2). Ehleringer & Pearcy (1983) reported a larger systematic variability in the quantum yield for CO₂ uptake among C₄ species (α_4), and in accordance with their findings we set α_4 to 0.067 and 0.062 mol mol^{-1} for C₄ grasses and maize, respectively. The value of the curvature parameter, θ_j , that acts to smooth the transition between J_m and APAR (Eq. A4), has been taken to be 0.7 (De Pury & Farquhar, 1997). The fitted values for the parameters θ_3 , θ_4 , β_3 , and β_4 , which control the degree of co-limitation between C₃ and C₄ photosynthetic rate limitations (Eq. A6) are from Collatz et al. (1991) and Collatz et al. (1992).

The Michaelis-Menten coefficients of Rubisco activity for CO₂ (K_c^{25}) and O₂ (K_o^{25}), respectively, and the CO₂ compensation point in the absence of dark respiration (Γ^{*25}) are thought to be intrinsic properties of the Rubisco enzyme. While expected to remain similar among higher plants (von Caemmerer et al., 1994) values reported in the literature at a reference temperature of 25 °C vary considerably. The values used here were determined from leaf gas exchange measurements on tobacco (Bernacchi et al., 2001) and are similar to values reported by Farquhar et al. (1980). The photosynthetic rate constants defined at a reference temperature of 25 °C (V_m^{25} , J_m^{25}) were adjusted with leaf temperature using energies of activation (E_a) and deactivation (H_d) derived as the average of gas exchange data compiled from 36 plant species (Kattge & Knorr, 2007). Activation energies for K_c^{25} , K_o^{25} and Γ^{*25} were adopted from Bernacchi et al. (2001).

4.4. Seasonal variations in photosynthetic efficiency

Considering temporal trends or physiological changes in V_m^{25} has been shown to be important for determining the seasonality and magnitude of the net CO₂ assimilation rate for deciduous broad-leaved trees (Wilson & Baldocchi, 2000; Kosugi et al., 2003; Xu & Baldocchi, 2003). These studies generally reported 1) a rapid increase in V_m^{25} during leaf expansion and development, 2) maximum values of V_m^{25} during the early stages of leaf maturity, and 3) a fairly rapid decrease in V_m^{25} during leaf senescence irrespective of species type. Flux tower studies also suggest that LUE changes with time in the growing season for deciduous forest and agricultural sites and that a decline in LUE towards the end of the growing season is associated with a decrease in foliar nitrogen concentration (Turner et al., 2003). Leaf nitrogen and chlorophyll content are significantly correlated with LUE (Gitelson et al., 2006) and V_m^{25} (Nijs et al., 1995) and recently Houborg et al. (2008) reported seasonal trends in leaf chlorophyll for a corn field that resembles the trends in photosynthetic capacity observed by Wilson & Baldocchi (2000) and Kosugi et al. (2003) for various species in a temperate deciduous forest stand. During model testing we also ran the models with seasonally changed V_m^{25} and β_n data for the agricultural and deciduous forest sites. For this purpose, V_m^{25} and β_n were assumed to scale linearly with green leaf area index ($L \times f_g$) from a minimum ($V_{m,min}^{25}$, $\beta_{n,min}$) during leaf emergence or complete senescence to a maximum ($V_{m,max}^{25}$, $\beta_{n,max}$) at peak green leaf area index (L_{max})

$$V_m^{25}(t) = V_{m,min}^{25} + \frac{L \times f_g}{L_{max}} (V_{m,max}^{25} - V_{m,min}^{25}) \quad (1)$$

$$\beta_n(t) = \beta_{n,min} + \frac{L \times f_g}{L_{max}} (\beta_{n,max} - \beta_{n,min}) \quad (2)$$

4.5. Respiration corrections

The CO₂ fluxes or net ecosystem exchange rates (if the CO₂ fluxes have been corrected for storage) measured at the flux tower sites incorporate respiratory contributions from leaves (R_d), stems/bole (R_b) and soil/roots (R_s). R_d and R_b are implicitly factored into the net CO₂ uptakes calculated by the LUE-based canopy sub-model as the nominal LUE values are based on estimates of aboveground and belowground net primary productivity. In the leaf-scaled sub-model, leaf growth and maintenance respiration are accounted for by the temperature dependent dark respiration rate (Eq. A13) but there is no correction for bole respiration that can be an important component of total autotrophic respiration in forests (Amthor, 1989). Bole respiration at the two forested sites (BH and WB) was computed using the equation (e.g. Edwards & Hanson, 1996):

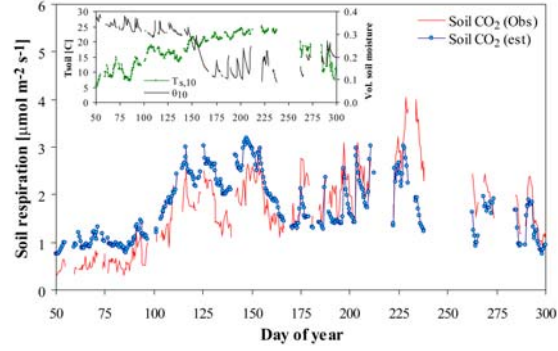


Fig. 2. Comparison of predicted and measured soil surface CO₂ fluxes at the Chesnut Ridge deciduous forest site. Estimates were based on the empirical soil respiration model developed by Norman et al. (1992) that takes into consideration the effect of root density, soil temperature and soil humidity (see insert).

$$R_b = R_b^{10} Q_{10}^{(T_b - 10)/10} \quad (3)$$

where R_b^{10} is the bole respiration rate at 10 °C, Q_{10} is the relative increase in respiration rate for a 10°C increase in temperature, and T_b is the bole temperature. R_b^{10} at WB was fixed to 0.43 $\mu\text{mol m}^{-2} \text{s}^{-1}$ according to Baldocchi (1997) and Edwards & Hanson (1996) and this value was also assumed representative for the ponderosa pine site (BH) (Ryan et al., 1995). The temperature sensitivity of R_b was modeled using a Q_{10} value of 2 (Amthor, 1989) and T_b was approximated as the average of the 10 cm soil temperature and air temperature.

The bulk of total ecosystem respiration originates from belowground autotrophic (i.e. roots) and heterotrophic (i.e. microbial) respiration. In order to compare the estimated canopy CO₂ uptakes with the flux measurements, this soil respiration component (upward flux positive by convention), must be added to the net ecosystem exchange rate measurements. The empirical soil respiration model developed by Norman et al. (1992) in a tall-grass prairie in Kansas has demonstrated effectiveness in reproducing observed soil respiration fluxes in grassland, prairie and agricultural ecosystems (Wagai et al., 1998; Anderson et al., 2008) with root-mean-square deviations on the order of 1 $\mu\text{mol m}^{-2} \text{s}^{-1}$. The model includes the effect of soil temperature ($T_{s,10}$) and volumetric soil moisture content (W_{10}) near the surface (10 cm) and the density of roots in the form of a surrogate variable, the leaf area index (L), as described by

$$R_s = (a + b \times L) W_{10} \exp(0.069(T_{s,10} - 25)) \quad (4)$$

where a and b are site-specific regression constants given as 0.135 and 0.054, respectively for the tall-grass prairie site in Kansas (Norman et al., 1992). The applicability of Eq. 4 for reproducing forest floor CO₂ respiration fluxes was tested using hourly chamber measurements from the base of the Chestnut Ridge flux tower located in deciduous forest in proximity to

Table 5. Quantitative measures of the overall performance of the LUE-based (lue) and scaled-leaf (mec) versions of ALEX in estimating half-hourly and daily integrated carbon and latent heat fluxes. The statistics are representative of daytime hours with vegetation on the ground (APAR > 10 $\mu\text{mol m}^{-2} \text{s}^{-1}$).

Flux	Vegetation	Half-hourly validation statistics								Daily integrated validation statistics							
		N	O	RMSD		MBE		R ²		N	O	RMSD		MBE		R ²	
				lue	mec	lue	mec	lue	mec			lue	mec	lue	mec		
A _c	Soybean	6545	15.3	5.4	6.4	1.1	0.8	0.82	0.72	251	31.3	6.5	7.6	2.3	1.6	0.89	0.82
	Corn	7161	19.1	8.5	9.3	4.2	4.9	0.84	0.82	274	37.0	12.5	14.2	8.8	10.2	0.89	0.85
	Grassland (AG)	18210	2.2	2.4	2.7	0.8	0.8	0.63	0.68	785	3.8	3.4	3.7	1.3	1.4	0.80	0.82
	Grassland (FP)	10355	5.1	2.9	3.0	0.4	0.3	0.41	0.44	367	11.3	3.8	4.6	0.7	0.7	0.66	0.61
	Grassland (GC)	12640	13.1	4.0	4.7	-1.1	-0.5	0.68	0.56	530	24.7	5.6	5.6	-2.1	-1.0	0.68	0.67
	Conifer	10295	5.7	3.2	3.5	0.6	0.6	0.44	0.33	388	12.1	4.1	4.5	1.1	1.0	0.40	0.34
	Deciduous forest	7622	14.0	9.1	9.0	3.7	0.8	0.61	0.45	309	26.6	10.7	9.9	4.1	1.5	0.78	0.81
LE	Soybean	7591	183	59	56	10	7	0.85	0.87	288	8.5	1.8	1.4	0.5	0.3	0.81	0.89
	Corn	7980	174	56	56	-3	7	0.86	0.86	304	7.8	1.6	1.7	-0.1	0.4	0.87	0.85
	Grassland (AG)	20776	62	34	41	6	16	0.77	0.72	897	2.5	0.8	1.1	0.2	0.7	0.89	0.82
	Grassland (FP)	12451	91	50	48	15	13	0.72	0.71	446	5.6	1.7	1.7	0.8	0.7	0.77	0.81
	Grassland (GC)	13651	167	45	53	8	-5	0.87	0.82	550	7.4	1.3	1.4	0.3	-0.3	0.83	0.80
	Conifer	10630	111	58	60	-20	-12	0.65	0.59	404	5.2	1.7	1.6	-1.0	-0.6	0.69	0.66
	Deciduous forest	8037	181	80	83	36	23	0.79	0.73	321	8.0	2.2	2.1	1.2	0.9	0.78	0.80

N is the number of observations, O is the mean of the observations, RMSD is the root-mean-square difference between model estimates and measurements, MBE is the mean bias error (if negative the model underestimates measurements), and R² is the coefficient of determination. O, RMSD and MBE have units of $\mu\text{mol m}^{-2} \text{s}^{-1}$ (A_c) and W m⁻² (LE) at the half-hourly time scale, and units of g C m⁻²

the Walker Branch flux tower. Fig. 2 shows a comparison of predicted and measured soil surface CO₂ fluxes averaged over 12 hour intervals (6 a.m. - 6 p.m., 6 p.m. - 6 a.m.). Model fitting yielded values of 0.061 and 0.022 for the a and b regression coefficients, respectively, which corresponds to a ~45% reduction of the original parameter values. The recalibrated model generally captures fluctuations caused by variations in soil temperature and soil moisture (see insert in Fig. 2) with a root-mean-square difference (RMSD) of only 0.53 $\mu\text{mol m}^{-2} \text{s}^{-1}$ for the year 2006. Model predictions also compared well with observations made during 2007 (RMSD = 0.85 $\mu\text{mol m}^{-2} \text{s}^{-1}$). The refitted model was also applied to the BH dataset assuming similarity in the magnitudes of soil respiration at some reference soil temperature and soil moisture content for these two forest ecosystems, while Eq. 4 with the original coefficients was used for the grassland and agricultural sites.

5. Model validation and intercomparisons

5.1. Carbon and latent heat fluxes

The LUE-based and scaled-leaf versions of ALEX were run using meteorological forcing and leaf area index data acquired at half-hourly intervals at each of the seven flux tower sites (Table 1). The full set of model parameterizations is listed in Table 2 and seasonally fixed values of β_n and V_m^{25} were used for these simulations. The overall agreement between net carbon assimilation and evapotranspiration fluxes simulated by ALEX and eddy covariance measurements is quantified in Table 5. The model performances are assessed using the root-mean-square difference (RMSD), mean-bias-error (MBE), and coefficient of determination (R²) statistical descriptors and

represent the average performance over the entire period of flux simulations. The flux comparisons have been restricted to daytime hours with vegetation on the ground (APAR) > 10 $\mu\text{mol m}^{-2} \text{s}^{-1}$ to facilitate an effective inter-comparisons of the two canopy sub-models (ALEX simulations at nighttime do currently not differ between the two versions). Both canopy sub-models do reasonably well at reproducing the observed magnitudes and variances of carbon and water vapor exchange on half-hourly and daily time-scales considering the simplicity of the ALEX modeling framework and the generality of the model parameterizations. Half-hourly carbon flux simulations by the LUE-based sub-model account for 82 -

Table 6. Coefficient of determinations (R²) of the LUE (lue) and scaled-leaf (mec) based versions of ALEX in estimating hourly carbon and latent heat fluxes when the flux data have been sorted by hour and averaged for 10-day periods. The statistics are representative of daytime hours with vegetation on the ground (APAR > 10 $\mu\text{mol m}^{-2} \text{s}^{-1}$).

Flux	Vegetation	R ²	
		lue	mec
A _c	Soybean	0.90	0.87
	Corn	0.89	0.88
	Grassland (AG)	0.73	0.71
	Grassland (FP)	0.56	0.55
	Grassland (GC)	0.81	0.75
	Conifer	0.70	0.49
	Deciduous forest	0.54	0.44
LE	Soybean	0.88	0.91
	Corn	0.93	0.93
	Grassland (AG)	0.90	0.85
	Grassland (FP)	0.80	0.78
	Grassland (GC)	0.91	0.89
	Conifer	0.80	0.75
	Deciduous forest	0.86	0.82

84 %, 41 – 68 %, and 44 – 61 % of the variance in measurements from agricultural, grassland, and forest

sites (Table 5). While carbon flux simulations by the scaled-leaf model are comparable in accuracy, the

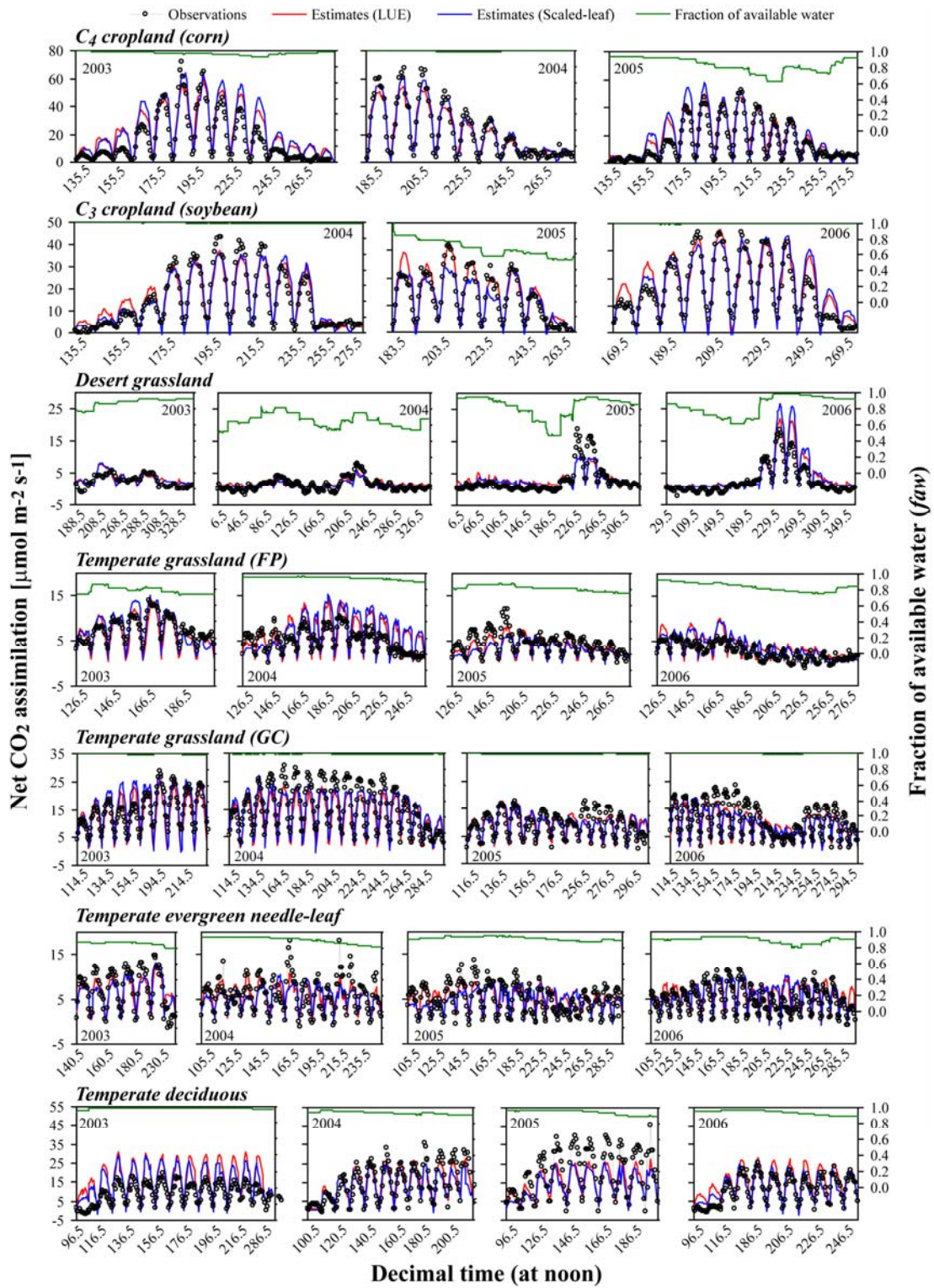


Fig. 3. These figures demonstrate the ability of the scaled-leaf and LUE-based models to reproduce temporal (diurnal, seasonal and inter-annual) patterns and magnitudes of CO₂ exchange over periods of 3 – 4 years at each flux tower site.

flux validation generally yielded slightly lower R^2 values and slightly higher RMSDs. Both models tend to overestimate carbon fluxes at the soybean (MBE = $0.8 - 1.1 \mu\text{mol m}^{-2} \text{s}^{-1}$), corn (MBE = $4.2 - 4.9 \mu\text{mol m}^{-2} \text{s}^{-1}$) and deciduous forest sites (MBE = $0.8 - 3.7 \mu\text{mol m}^{-2} \text{s}^{-1}$). The agreement (i.e. R^2) between model calculations and measurements improve markedly when comparing daily integrated carbon flux data (Table 5). Kellomäki and Wang (2000) and Anderson et al. (2000) also saw an improvement in the coefficient of determination when averaging hourly flux data between sunrise and sunset. The fact that CO_2 fluxes were not corrected for storage possibly amplify discrepancies between observed and modeled flux quantities at the half-hourly time scale and may explain the significant change in R^2 from 0.45 to 0.81 at the deciduous forest site reported for daily integrated fluxes generated by the scaled-leaf model (Table 5). The correlation between measurements and estimates remains poor for the ponderosa pine site in Black Hills. Law et al. (2000) and Anderson et al. (2000) also reported low R^2 values for evergreen needle-leaf forest.

For the purpose of model testing, it has been argued that eddy-flux measurements of carbon and water should be averaged by time to reduce random errors in the measurements and the natural variability that is associated with individual periods (Moncrieff et al., 1996; Baldocchi and Wilson, 2001). Sorting the fluxes by hour and averaging them over 10 day periods improve the R^2 statistics of the carbon and latent heat flux simulations significantly for most sites (Table 6). The carbon flux R^2 remains low for the grassland (FP) and deciduous forest sites but noteworthy is the improved performance of the latent heat flux simulations for all sites (Table 6) where linear regression now yields coefficient of determinations ranging from 0.80 to 0.93 (LUE-based simulations). Overall the LUE-based model simulations are seen to account for more of the variance in the measurements than the scaled-leaf model simulations.

5.2. Temporal variations in carbon fluxes

The statistics reported in Table 5 and 6 may hide seasonal and interannual variations in the agreement between model simulations and eddy covariance measurements. Fig. 3 demonstrates the ability of the two models to reproduce temporal (diurnal, seasonal and interannual) patterns and magnitudes of net CO_2 assimilation (A_c) over periods of 3 – 4 years at each flux tower site. For illustrative purposes, each diurnal segment represents flux data averaged by hour (day-time only) over 10-day intervals. The year long records at the desert grassland site were averaged over 20-day intervals. Since the data have not been gap-filled the flux records are not complete for all years. The time evolution of the modeled fraction of available water (f_{aw}) is over-plotted to illustrate periods with soil-water-limited CO_2 assimilation rates.

The biases at the corn and soybean sites reported in Table 5 are the result of overestimations early in the season during leaf expansion (~doy 130 - 180), toward the end of the leaf maturity stage and during leaf senescence (~doy 220 →) (Fig. 3). For C_3 cropland the discrepancy between modeled and measured fluxes early in the season is largest for the LUE-based model while the opposite is true for C_4 cropland. Both models are generally successful in reproducing the magnitude of A_c during the leaf maturity stage. Although not as unequivocal overestimations early in the growing season can also be identified in the 2003 and 2006 flux record at the deciduous forest site. The seasonal trends in A_c for the corn, soybean and deciduous forest sites may be the result of seasonal dynamics in photosynthetic efficiency that has been shown to vary over the course of a season as leaves expand, age and senescence (Wilson et al., 2000; Kosugi et al., 2003; Xu & Baldocchi, 2003). Model runs with seasonally changed V_m^{25} and β_n are presented and discussed in section 5.4. The observed biases early in the season could also be related to seasonal variations in leaf respiration. Leaf respiration at 25°C is modeled as a constant fraction of V_m^{25} and is implicitly incorporated in the estimates of β_n based on seasonal or annual biomass accumulation, which makes both canopy sub-models unfit to reproduce the observed tendency towards peak respiration rates during leaf development and gradually declining leaf respiration as leaves mature (Xu & Baldocchi, 2003; Wilson et al., 2001). However, the scaled-leaf model is expected to reproduce some of the temporal dynamics of leaf respiration due to the modeled non-linear dependence on leaf temperature (Eq. A13).

Midday and early afternoon depressions in assimilation rates modeled by the scaled-leaf model are particularly pronounced during the 2005 dry spell (~doy 205 – 225) at the soybean site. Air temperatures were typically around 30°C and winds were generally very calm ($< 2 \text{ m s}^{-1}$) which resulted in modeled sunlit leaf temperatures on the order of 40 - 45°C. At these fairly extreme temperatures the applied peaked temperature response functions (Eq. A14) cause deactivation of V_m and J_m at rates determined by their respective deactivation energies (H_d , Table 2). The kinetic rate constants adopted here assume an optimum temperature for photosynthesis (T_{opt}) of 32°C and a gradual decrease in activity above this temperature. However the large flux underestimation during this period suggests that T_{opt} should be higher for soybean. In fact Kattge & Knorr (2007) and Medlyn et al. (2002) reported a T_{opt} of 41°C for soybean cultivars. Fig. 4a demonstrates the effect of the deactivation term in the generalized temperature response function on A_c for selected flux records averaged by hour over 10-day periods. Hourly carbon fluxes are seen to increase by up to $\sim 12 \mu\text{mol m}^{-2} \text{s}^{-1}$ if the deactivation is neglected and V_m and J_m are allowed to keep increasing at the rate determined by their respective activation energies (see insert for

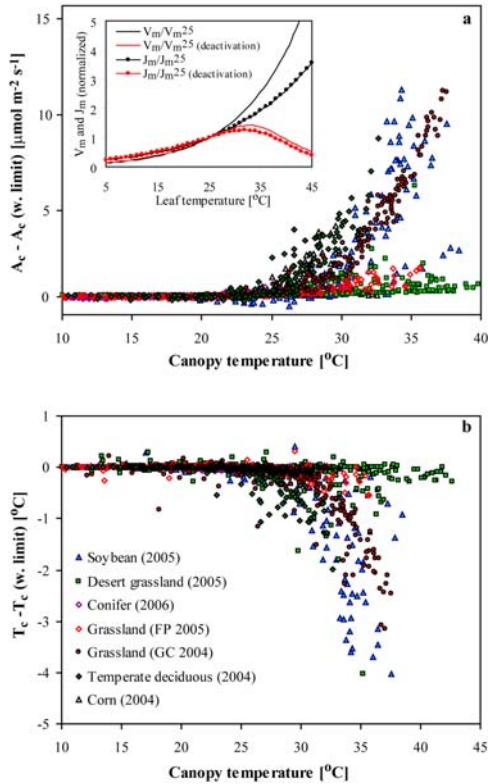


Fig. 4 a) The effect of a gradual deactivation of V_m and J_m on CO_2 assimilation (A_c) for selected flux records. The insert depicts normalized temperature response function with and without the deactivation term. b) The effect of the deactivation on simulated canopy temperatures.

normalized temperature response functions with and without the deactivation function). Significant deviations in flux estimates begin to occur at canopy temperatures (T_c) exceeding 25°C as the peaked (deactivation) and regular (no deactivation) Arrhenius functions diverge. The magnitude of the flux divergences is positively correlated with T_c (Fig. 4b) but also depends on the environmental controls and leaf area index in particular. The very high canopy temperatures modeled at the soybean, grassland (GC) and deciduous forest sites are probably the result of a T_c feedback loop initiated by the gradual deactivation of photosynthesis at canopy temperatures above 32°C ; The reduced rate of CO_2 assimilation will cause a higher stomatal resistance and lead to a decrease in the latent heat flux and a greater fraction of the available energy partitioned into sensible heating which will then increase T_c and thus decrease A_c even further. The initiation of temperature limitation on photosynthesis appear to be unfortunate for the soybean, grassland (GC) and deciduous forest sites as the coefficient of variance (R^2) decrease from 0.88, 0.88, and 0.73 (without deactivation) to 0.83, 0.79, and 0.61 (with deactivation), respectively. Whether temperature limitation of V_m and J_m occur is debated. Kattge & Knorr (2007) demonstrated a tendency for an ac-

climation response of V_m and J_m to growth temperatures with optimum temperatures of 36 species ranging from 20 to 50°C . Dreyer et al. (2001) reported the temperature optima of seven temperate tree species to range between 35.9 and above 45°C whereas Bernacchi et al. (2001) found that the addition of a deactivation term was unnecessary at temperatures $< 40^{\circ}\text{C}$. Clearly the temperature dependency of Rubisco kinetic properties is the matter of considerable uncertainty. The use of species-specific temperature acclimation response functions may be critical for a successful implementation of the scaled-leaf model.

Photosynthesis may also be inhibited by low temperatures. At the northerly needle-leaf forest site in Black Hills, Montana air temperatures occasionally dropped below 5°C in the beginning of the 2005 flux record (Fig. 3). As a consequence CO_2 fluxes simulated by the scaled-leaf model became co-limited by the carbon compound export limited transport rate (A_s) (Eq. A5) which resulted in significant underestimation of A_c . The LUE-based model estimates on the other hand provided an excellent fit with measurements during this period. Low temperature inhibition was also in effect during 2006 ($< \text{doy } 135$ and $> \text{doy } 275$) but here the scaled-leaf model simulations corresponded well with measurement while the LUE-based model estimates were positively biased.

Both canopy models do a reasonable job at capturing seasonal and year-to-year variations in A_c at the three grassland sites (Fig. 3). At the desert grassland site vegetation growth is impaired by soil water deficits ($f_{aw} < 1$) throughout much of the year but respond rapidly to rainfall events during the late summer monsoon season. The flux underestimation in 2005 and overestimation in 2006 during peak vegetative growth could be related to uncertainties in the estimation of leaf area index (L) that presumably reached maximum values of 1.1 and 3.1, respectively. The time-series of L were deduced using empirical exponential functions between L and tower-derived NDVI (Wilson & Meyers, 2007). The derived values of L were not verified against field measurements for the grassland sites and a value of 3.1 appear high for this environment as Wilson & Meyers (2007) list a maximum L of 0.6 for the Audubon desert grassland site based on data from 2002 - 2005. Also the L values are essentially point measurements and may not be spatially representative of the flux tower footprint (source area) at all times. Spatial heterogeneity in L in the immediate vicinity of the flux towers at the grassland sites could provide partial explanations for the periodic fairly significant discrepancies between flux simulations and measurements. Differences in flux footprint may also play a significant role at the evergreen needle-leaf forest site in Black Hills as this site is quite heterogeneous and characterized by large open spaces (Wilson & Meyers, 2007).

Uncertainties related to the estimation of f_{aw} could be another significant source for biased flux simulations. While simulated soil water stress at the

Fort Peck grassland site during 2003, 2005 and 2006 reduce A_c to provide reasonable agreements with the eddy flux data, f_{aw} simulations during 2004 indicate

fairly ample soil moisture conditions ($f_{aw} \sim 0.95$) causing the carbon fluxes to be overestimated by 31% on average. The site received a similar amount of

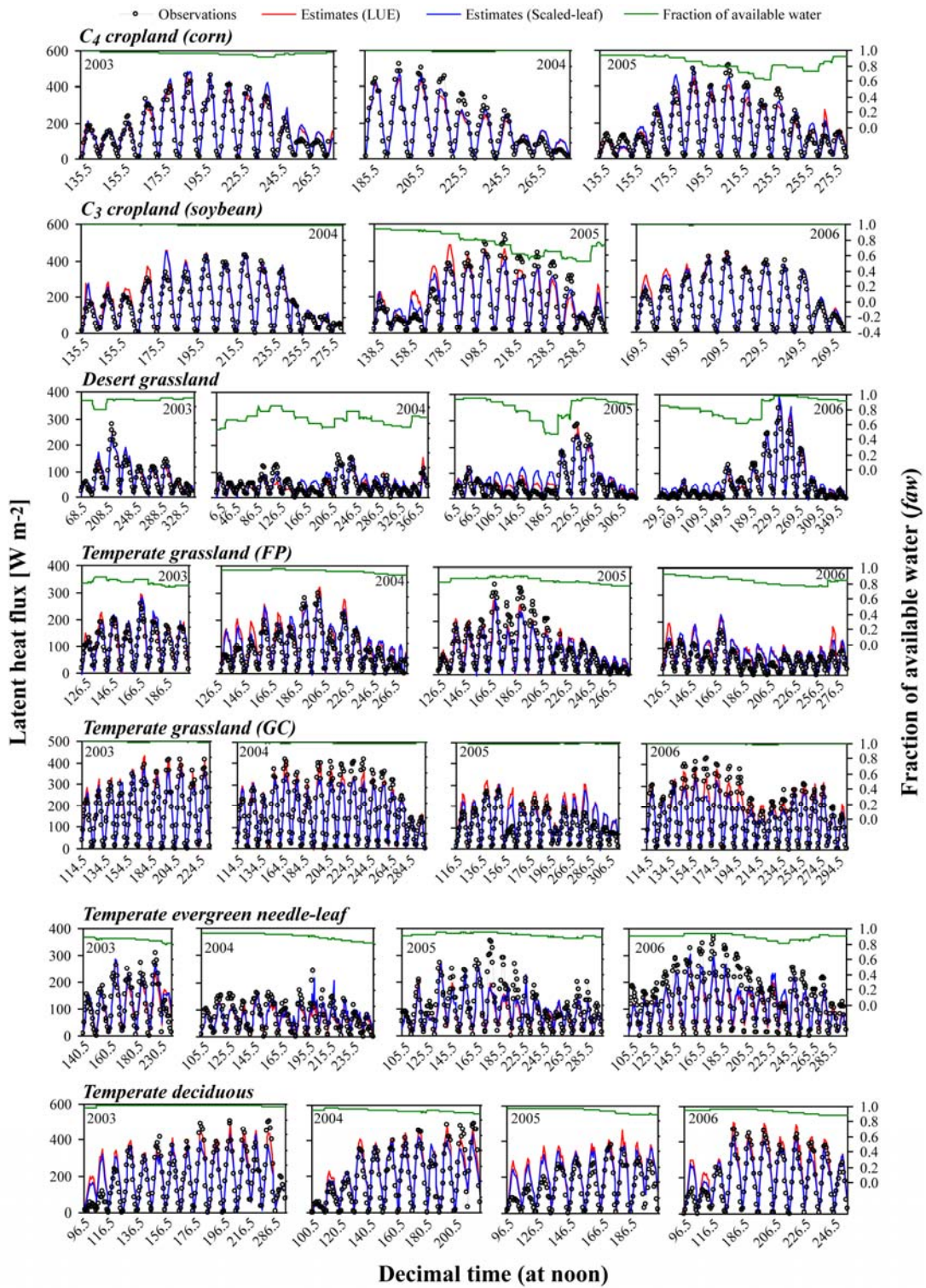


Fig. 5. These figures demonstrate the ability of the scaled-leaf and LUE-based models to reproduce temporal (diurnal, seasonal and inter-annual) patterns and magnitudes of latent heat exchange over periods of 3 – 4 years at each flux tower site.

precipitation (~200 mm) during the May – September growing season in all 4 years. However, the initial soil moisture profile used as input to the soil transport module in 2004 was characterized by comparatively higher soil moisture contents due to a rainfall event just prior to the start of the simulations. Consequently, the soil transport module modeled a too slow depletion of soil moisture from the root zone (not shown). The estimation of f_{aw} depends heavily on the setting of the wilting point and field capacity soil moisture content which are linked to soil type. In the current model setup only a single soil layer with generalized hydraulic and thermal properties is assumed and the very simplistic treatment of soil processes can easily cause errors in the estimation of f_{aw} and thus canopy fluxes.

Carbon flux simulations at the deciduous forest site at Walker Branch diverge considerably from observations during 2003 and 2005 in particular. Simulations by the LUE-based and scaled-leaf models are generally comparable in magnitude and tend to track each other closely during the morning hours up till around midday. The afternoon reduction in rates of CO₂ assimilation simulated by the scaled-leaf model is probably related to partial deactivation of V_m and J_m as a result of high temperatures as discussed above. Measured fluxes are comparatively low during the 2003 growing season despite it being the wettest season (~830 mm compared to ~650 during 2004 – 2006) and experiencing relative humidities greater than 40% throughout the growing season. Variations in the extent and composition of the upwind source area (i.e. footprint) of the fluxes measured at the tower could be a significant source of variance between measurements and model estimates as the composition of species viewed by the tower is likely to change with wind direction and atmospheric stability in this mixed forest stand. The distribution of wind directions did vary between 2003 and 2005. In 2003 winds primarily originated from either north-northeasterly or south-southwesterly directions while the wind regime during 2005 was very variable. While forest species may differ to a considerable extent in their biochemical capacity to assimilate CO₂ from the atmosphere (Wullschleger, 1993), species-specific differences in photosynthetic efficiency have been shown to be not so important for determining the energy budget (Anderson et al., 2008) and the latent heat fluxes are reasonably reproduced in both years (Fig. 5). However an adjustment of β_n and V_m^{25} may be required to accommodate inter-annual variations in the species composition viewed by the flux tower and appear to be critical for modeling year-to-year carbon fluxes accurately at this site.

5.3. Temporal variations in latent heat fluxes

Fig. 5 demonstrates the ability of the two canopy sub-models to reproduce temporal patterns and magnitudes of latent heat exchange over the course of

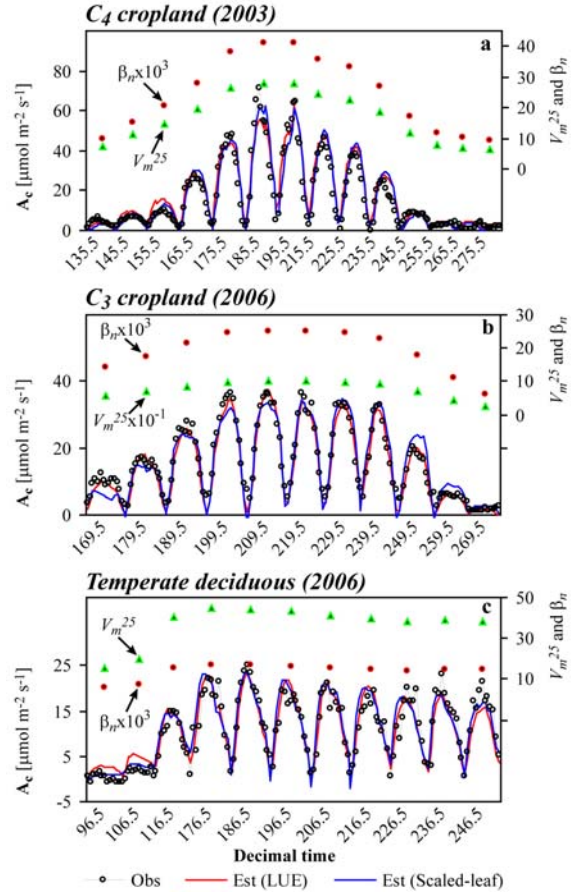


Fig. 6. Comparison between carbon flux measurements and simulations based on seasonally changed V_m^{25} and β_n data for corn (a), soybean (b), and deciduous forest (c) sites.

several years. As is also evident from the statistics in Table 5 and 6, the latent heat fluxes are generally reproduced with high fidelity. While LE is calculated using the same formalism (Eq. A11 and Eq. B1) the input stomatal resistance will reflect changes in A_c that is calculated based on very different equation sets (Table A1 and Table B1). Additionally, in the scaled-leaf model the derived LE is the sum of contributions from sunlit and shaded leaf fractions. Nevertheless, flux simulations by the two models tend to be highly inter-correlated. The largest divergences between simulations by the two models occur early in the season at the soybean, Fort Peck temperate grassland, and temperate deciduous forest sites and they generally correlate with the carbon flux divergences. Inter-correlation of A_c and LE is expected as they are linked by the stomatal conductance that simultaneously regulate the conflicting demands of allowing CO₂ assimilation by leaves and minimizing the water loss from the leaves to the environment. Noteworthy, is the overall good performance of the latent heat flux simulations at the deciduous forest site considering the difficulties associated with reproducing inter-annual variations in the carbon flux at this site (Fig.

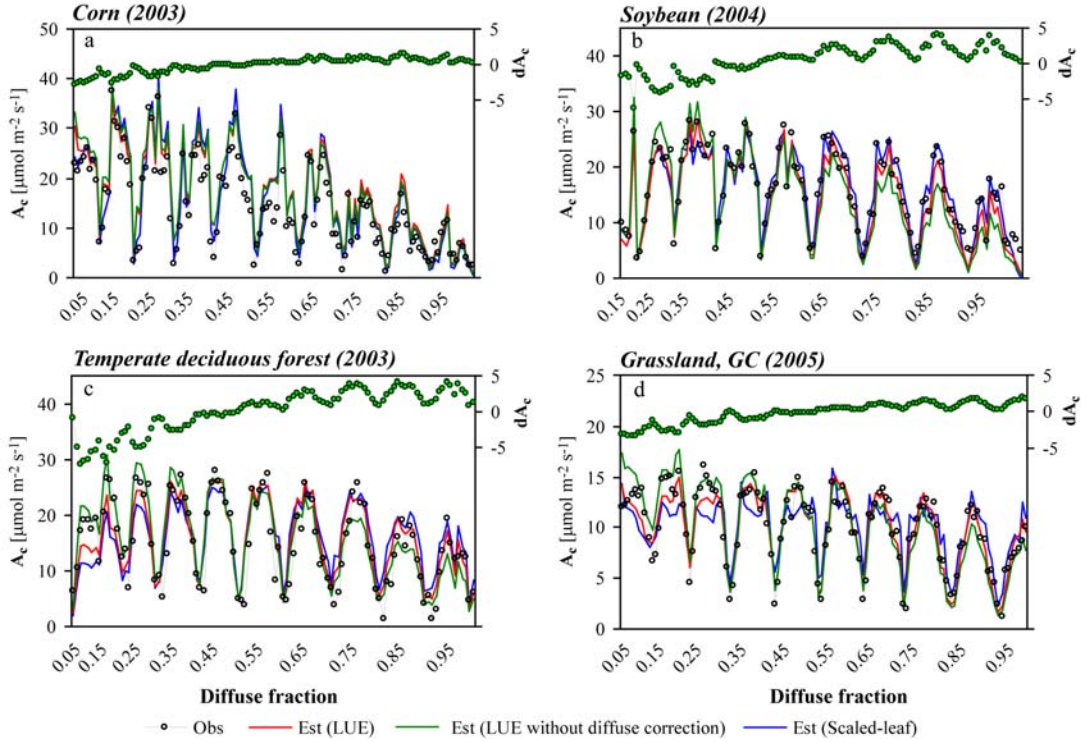


Fig. 7. The correspondence between hourly carbon flux simulations and measurements when sorted as a function of the fraction of diffuse radiation. Each segment represents the averaged hourly flux response during conditions throughout the growing seasons where the diffuse radiation was within the specified interval.

3). Reduced CO_2 assimilation rates as a result of deactivation of V_m and J_m (section 5.2) will initially decrease LE due to a decrease in stomatal conductance. However the associated leaf temperature increase (Fig. 4) will increase the vapor pressure deficit and thereby counterbalance the stomatal conductance effect (Eq. A11). The sensitivity analysis in section 5.7 also suggests that uncertainties related to A_c estimation generally have a reduced effect on LE.

The occasionally high discrepancies between estimated and measured flux quantities early in the seasons may be related to overestimates of the green leaf area index prior to leaf emergence (~ 1.0 , ~ 0.5 , and ~ 0.2 at the temperate deciduous, soybean, and Fort Peck grassland sites, respectively) or may reflect uncertainties related to the estimation of soil evaporation.

The Bowen-ratio corrected latent heat fluxes were on the order of 10 – 35 % higher than the eddy flux measurements at the cropland, evergreen needle-leaf and grassland sites except for Fort Peck where corrected fluxes were ~ 10 % less. At the deciduous forest site a latent heat flux increase of $\sim 65\%$ was required to sum H and LE to the available energy ($R_n - G$) while retaining the observed Bowen ratio which suggests significant energy storage within the forest stand. The Bowen-corrected fluxes provided the best fit with measurements at all sites. Residually corrected latent heat fluxes (i.e. $\text{LE} = R_n - H - G$) were be-

tween 0 – 40 % larger than the Bowen-ratio corrected fluxes and resulted in the highest RMSDs between measured and estimated fluxes at the Black Hills, Goodwin Creek and Audubon sites (i.e. higher than when comparing uncorrected eddy flux observations and model estimates).

5.4. Seasonality in photosynthetic efficiency

Carbon flux simulations based on seasonally changed V_m^{25} and β_n data are illustrated for soybean, corn, and deciduous forest sites in Fig. 6. V_m^{25} and β_n were scaled linearly with green leaf area index using Eq. 1 and 2, respectively. $V_{m,min}^{25}$ and $\beta_{n,min}$ were parameterized as 15 % (corn and forest) and 40 % (soybean) of maximum V_m^{25} and β_n during green up, and set to zero during the late season decline corresponding to fully senescent leaf material (no photosynthetic activity). Maximum V_m^{25} and β_n correspond to the values listed in Table 2. Evidently, the fit between estimates and measurements is significantly improved at the cropland sites as a result of incorporating temporally varying V_m^{25} and β_n data (Fig. 6a and 6b). At the corn site the RMSD of the hourly simulations during 2003 was reduced from 11.6 to 6.4 $\mu\text{mol m}^{-2} \text{s}^{-1}$ for the scaled-leaf model and from 10.5 to 6.9 $\mu\text{mol m}^{-2} \text{s}^{-1}$ for the LUE-based model while R^2 values of ~ 0.95 were derived when regressing hourly data averaged over 10-day periods. Regression analy-

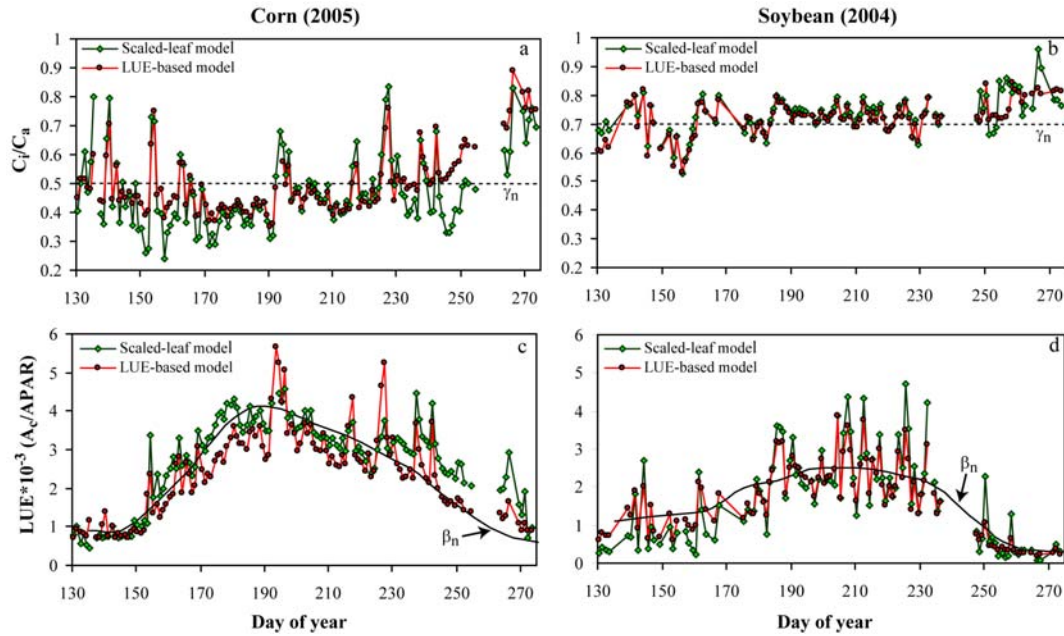


Fig. 8. Time-series of simulated ratios of intercellular to ambient CO₂ concentration (C_i/C_a) (a and b) and light-use efficiencies (LUE) (c and d) around noon for corn and soybean sites. Nominal values of C_i/C_a (γ_n) and LUE (β_n) are over-plotted with dotted and solid lines, respectively.

sis based on hourly averaged flux data at the soybean site yielded R^2 of 0.91 and 0.97 for the scaled-leaf and LUE-based models, respectively. Significant performance improvements were also observed for the latent heat fluxes (not shown). At the forest site, the scaled-leaf model was run without the deactivation term in the temperature response functions for V_m and J_m to facilitate a reasonable fit with the flux measurements. In this seasonal parameterization, the optimum phase of photosynthesis occur in June at the forest site and V_m and β_n only diverge slightly from their optimal values during the remainder of the depicted flux record due to only moderate variations in L during this stage of leaf maturity (Fig. 6c). The flux record at the forest site is too short to capture the more rapid decline in photosynthetic capacity during the period of autumnal senescence reported in a number of studies (Xu & Baldocchi, 2003; Wilson et al., 2001; Kosugi et al., 2003). Wilson et al (2001) reported more dynamics in V_m over the growing season in a deciduous forest stand and included leaf age specifically as a reducing factor after the spring maximum in V_m . Evidently, some consideration of temporal changes in V_m and β_n is needed to reproduce the carbon fluxes with high fidelity at these sites. The simplified seasonal parameterization procedure demonstrated here varies V_m and β_n during leaf development and senescence where changes in photosynthetic efficiency are most likely to occur and is well suited to application over large regions as green leaf area index can be derived with reasonable accuracy from remote sensing.

5.5. Impact of light environment

CO₂ assimilation efficiency is known to increase under more diffuse radiation conditions (e.g. Gu et al., 2002) as diffuse radiation is more uniformly distributed over leaves in a canopy causing a smaller fraction of the leaves to experience light saturation. This phenomenon is treated very differently by the two canopy models. The scaled-leaf model responds to an increase in the fraction of PAR that is diffuse (f_{dif}) by partitioning a greater fraction of the PAR to the shaded fraction of leaves in the canopy. Shaded leaves typically operate in Rubisco limited mode (i.e. not limited by light) and therefore have larger light-use efficiencies. In the LUE-based model the response to f_{dif} is based on simulations by the Cupid model (Norman & Arkebauer, 1991) that indicated a nearly linear response of LUE to f_{dif} (Eq. B8). Fig. 7 illustrates the correspondence between hourly carbon flux simulations and measurements averaged over the fraction of diffuse radiation. Each segment represents the averaged hourly flux response during conditions throughout the growing seasons where the diffuse radiation was within the specified interval (e.g. 0 – 0.1, 0.1 – 0.2). In most of the studied cases the scaled-leaf model reproduces A_c well during variable diffuse lighting conditions. The model underestimates fluxes at the grassland site around noon when the radiation above the canopy was mainly direct which likely reflect high temperature deactivation of V_m and J_m (section 5.2) as high temperature inhibition of photosynthesis is most likely to occur when the fraction of PAR absorbed by sunlit leaves is greatest. The

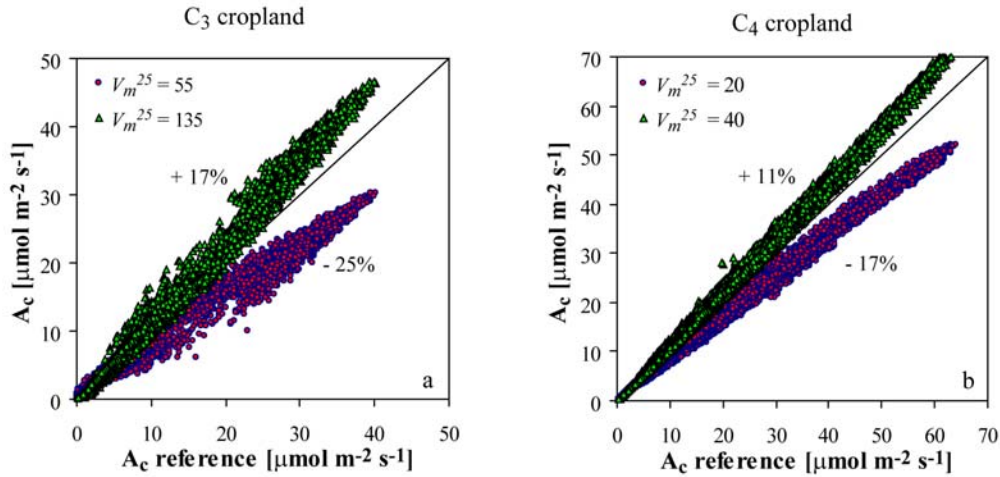


Fig. 9. The sensitivity of half-hourly carbon flux simulations by the scaled-leaf model to variations in V_m^{25} for crops with C_3 (a) and C_4 (b) photosynthetic pathways, respectively. The relative change in % in response to the applied changes is also shown.

fraction of PAR absorbed by the shaded fraction of the canopy increased from ~ 0.05 to ~ 0.6 when the light environment changed from mainly direct ($f_{dif}=0.05$) to mainly diffuse ($f_{dif}=0.95$).

The applied modification of β_n with changes in diffuse lighting is seen to be critical for matching flux simulations with measurements during conditions when more than 50% of the radiation is diffuse at the soybean, forest and grassland sites. The modification of β_n results in increases of up to $5 \mu\text{mol m}^{-2} \text{s}^{-1}$ in hourly averaged fluxes during mainly diffuse radiation conditions and decreases of up to $8 \mu\text{mol m}^{-2} \text{s}^{-1}$ during mainly direct radiation conditions (Fig. 7). The minimal effect of the β_n modification at the corn site reflects the fact that leaves of C_4 species saturate at higher light levels than leaves of C_3 species and this tendency is supported by the model results. The LUE-based model tends to perform slightly better than the scaled-leaf model during predominantly direct radiation conditions but still underestimates measurements at the deciduous forest site. ALEX uses a fairly simplistic analytical formalism to describe light interception by canopies (Goudriaan, 1977; Anderson et al., 2000) that not specifically treat the complexity of light penetration in forest stands (e.g. penumbral effects) which may result in underestimation of absorbed PAR and the fraction of absorbed PAR distributed on shaded leaves when radiation is primarily direct.

5.6. Intercomparisons of CO_2 concentration and light-use efficiency

Time-series of simulated ratios of intercellular to ambient CO_2 concentration (C_i/C_a) around noon are shown in Fig. 8a and c for corn and soybean sites. The C_i/C_a ratio (γ) simulated by the LUE-based model fluctuates around the nominal value of C_i/C_a (γ_n) in

response to changes in diffuse radiation conditions, stomatal conductance and soil water deficits. The LUE-based modeling paradigm assumes that the functional dependence of A_c on C_i becomes linearized on the canopy level (Anderson et al., 2000) and the derived γ values generally track the dynamics in γ simulated by the scaled-leaf model closely. The derived γ values are within the range you would normally expect for plants with C_4 and C_3 photosynthetic pathways (Wong et al., 1979). Changes in γ are directly reflected in the actual light-use efficiencies calculated as A_c/APAR (Fig. 8b and d). The magnitude of the change in actual LUE from the seasonally changed nominal value (β_n – the over-plotted black solid line) is on the order of ± 0.007 for the corn site and ± 0.009 for the soybean site. Evidently, LUE-based carbon models that don't take into consideration the C_i –LUE response may face serious issues in tracking day-to-day variations in CO_2 assimilation fluxes.

5.7. Sensitivity to variations in adjustable parameters

Discrepancies between model simulations and observations may also be attributed to the values used for the adjustable canopy parameters specific to each canopy sub-model (Table 2). The sensitivity of the models to variations in key parameters was examined by linearly regressing nominal run model output with simulation results obtained using new values of each parameter, while holding the others unchanged. The linear relationships were forced through zero intercept and the regression slopes were used to assess the average respond of the applied changes in parameter values on the simulation results. Table 7 and 8 present carbon and latent heat flux sensitivity results obtained when the adjustable parameters specific to

Table 7. Sensitivity of carbon and energy fluxes to variations in the adjustable parameters specific to each C₃ canopy sub-model, expressed as slopes of regressions lines. A slope greater than unity indicates that sensitivity run simulations overestimate reference run simulations. The sensitivity results were generated using the pattern of canopy development and environmental conditions observed during the 2004 growing season (May – September) at the Bondville (BV) soybean site.

C ₃ cropland	Parameter	Sensitivity range (max,min)	Deviation in fluxes from reference			
			Ac		LE	
			Max	Min	Max	Min
<i>Scaled-leaf</i>						
V_m^{25}	95 ± 40	1.17	0.75	1.05	0.91	
J_m^{25}/V_m^{25}	1.9 ± 0.4	1.04	0.94	1.01	0.98	
k_n	0.7 ± 0.3	0.98	1.02	0.99	1.01	
α_3	0.37 ± 0.07	1.10	0.89	1.03	0.97	
θ_j	0.7 ± 0.2	1.06	0.95	1.01	0.99	
θ_3	0.9 ± 0.1	1.18	0.92	1.05	0.97	
<i>LUE-based</i>						
β_n	0.024 ± 0.006	1.23	0.76	1.05	0.94	
γ_n	0.7 ± 0.1	0.84	1.23	0.96	1.05	

each C₃ and C₄ canopy sub-model were changed as indicated. The half-hourly model simulations were based on model runs encompassing the entire growing season at the corn and soybean sites and thus represent a wide range in environmental and phenological conditions. The sensitivity of carbon flux simulations to variations in V_m^{25} is showed graphically in Fig. 9a and b for crops with C₃ and C₄ photosynthetic pathways, respectively. Increasing V_m^{25} from 95 to 135 $\mu\text{mol m}^{-2} \text{s}^{-1}$ (C₃) and 30 to 40 $\mu\text{mol m}^{-2} \text{s}^{-1}$ (C₄) lead to a 17 % and 11 % rise in A_c, respectively, while decreases of 25 % and 17 % are produced when V_m^{25} is reduced to 55 and 20 $\mu\text{mol m}^{-2} \text{s}^{-1}$, respectively. The latent heat flux (LE) is less sensitive to variations in photosynthetic capacity (Table 7 and 8) as V_m^{25} acts indirectly on canopy transpiration through the stomatal conductance. Correspondingly, latent heat fluxes are seen to be significantly less sensitive to variations in the photosyn-

Table 8. As in Table 7 but using the pattern of canopy development and environmental conditions observed during the 2005 growing season (May – September) at the Bondville (BV) corn site.

C ₄ cropland	Parameter	Sensitivity range (max,min)	Deviation in fluxes from reference			
			Ac		LE	
			Max	Min	Max	Min
<i>Scaled-leaf</i>						
V_m^{25}	30 ± 10	1.11	0.83	1.03	0.95	
k/V_m^{25}	$20 \times 10^3 \pm 10 \times 10^3$	1.01	0.98	1.00	0.99	
k_n	0.7 ± 0.3	0.97	1.04	0.99	1.01	
α_4	0.062 ± 0.01	1.08	0.90	1.02	0.97	
θ_4	0.9 ± 0.1	1.12	0.94	1.03	0.98	
β_4	0.9 ± 0.1	1.03	0.98	1.01	0.99	
<i>LUE-based</i>						
β_n	0.042 ± 0.006	1.11	0.89	1.03	0.97	
γ_n	0.5 ± 0.1	0.87	1.19	0.97	1.04	

thetic parameters J_m^{25}/V_m^{25} , k_n , α_3 , θ_j , θ_3 , k/V_m^{25} , α_4 , θ_4 , and β_4 than are CO₂ assimilation rates (Table 7 and 8). The same tendency is evident in the sensitivity results for the LUE-based model (Table 7 and 8), which supports other studies (e.g. Anderson et al., 2008; Leuning et al., 1998) that suggest that the choice of key photosynthesis model parameters is not so important for determining energy fluxes accurately.

The quantum yield for electron transport (α_3) and CO₂ uptake by C₄ plants (α_4) are critical parameters in the scaled-leaf model as A_c is seen to change with ~10% when α_3 and α_4 are varied as shown. Adopted values for α_3 typically vary between approximately 0.18 and 0.40 (Wullschlegel, 1993; Harley et al., 1992; Medlyn et al., 2002; Leuning et al., 1998, Farquhar et al., 1980) and quantum yield may also exhibit seasonal patterns of variation (Gilmanov et al., 2005), which add to the uncertainty in their parameterization. Reported values of the J_m^{25}/V_m^{25} ratio vary widely from around 1.6 to ~3.3 (Medlyn et al., 2002; Kattge & Knorr, 2007; Leuning, 2002; Wohlfahrt et al., 1999; Wilson et al., 2001) and J_m^{25}/V_m^{25} has also been show to vary over the growing season (Wilson et al., 2000). While variability in J_m^{25}/V_m^{25} has been related to differences in plant type and climate, results remain inconclusive and the use of a fixed ratio could lead to serious model deficiencies for certain species or environments as modest variations in J_m^{25}/V_m^{25} (± 0.4) change A_c by approximately 5 % (Table 7). Increasing the C₃ and C₄ curvature (co-limitation) parameters (θ_3 , θ_4) from 0.9 to 1.0 leads to an 18 and 12 % increase in A_c, respectively, which makes the issue of the degree of co-limitation between electron transport (A_j) and Rubisco limited (A_c) CO₂ assimilation equally important to the parameterization of V_m^{25} . Interestingly, De Pury & Farquhar (1997) ignored the gradual transition between A_j and A_v completely arguing that co-limitation has little effect on C₃ canopy photosynthesis, as only a small fraction of leaves are near the transition to light saturation at any moment. In C₄ plants Collatz et al. (1992) observed a gradual saturation of A_c with respect to incident quantum flux which suggested significant co-limitation between A_j and A_v and a fitted curvature parameter significantly less than one.

In the LUE-based model parameterization, uncertainties are reduced to only two adjustable parameters that appear to be equally influential in modifying CO₂ assimilation rates (Fig. 10 and Table 7 and 8). The respond of A_c to the applied variations in nominal LUE (β_n) is approximately linear with characteristic changes of $\pm 23\%$ and $\pm 11\%$ for C₃ and C₄ plants, respectively while A_c is seen to be more sensitive to a decrease in nominal C_i/C_a (γ_n) than a corresponding increase in γ_n (Table 7 and 8). While β_n (when representing maximum light-use-efficiency for unstressed vegetation) appears to be a fairly conservative quantity within major vegetation classes based on the compiled estimates listed in Table 3, the tabulated

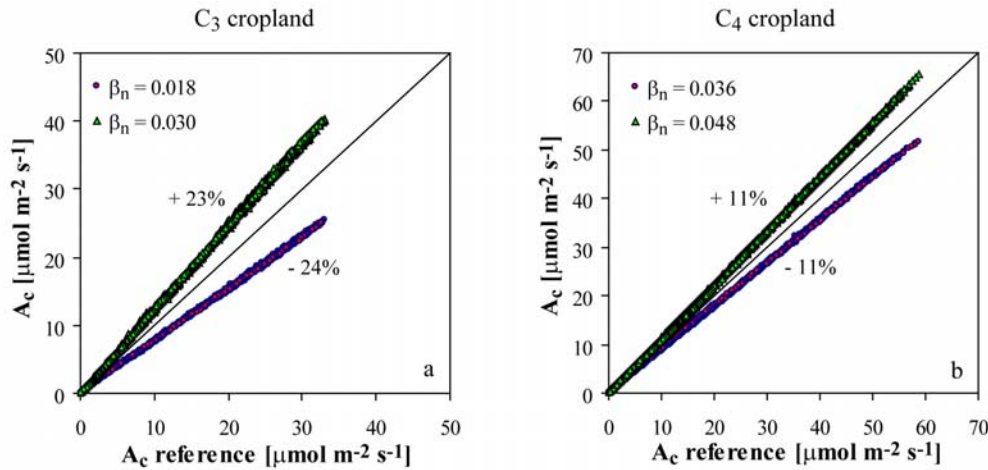


Fig. 10. The sensitivity of half-hourly carbon flux simulations by the LUE-based model to variations in nominal LUE (β_n) for crops with C₃ (a) and C₄ (b) photosynthetic pathways, respectively. The relative change in % in response to the applied changes is also shown.

standard deviations were based on a fairly small number of samples. Additional intra-class variability in β_n may arise as a result of e.g. variability in respiratory behavior (i.e. respiration to assimilation ratio), stand age and vegetation nutrient status. Also, estimates of β_n are associated with several sources of uncertainty and inconsistencies as discussed in detail by Gower et al. (1999). However, approximating realistic β_n and γ_n values for major vegetation groups appear as considerably more straightforward than specifying the large number of tunable leaf-scale parameters with acceptable accuracy for different species compositions and environments. Additionally, the scaled-leaf model is susceptible to errors in the leaf to canopy scaling assumptions whereas the LUE-based approach is constrained to the realm of observation (Jarvis, 1993).

6. CONCLUSION

‘Bottom-up’ (scaled-leaf) and ‘top-down’ (LUE-based) modeling paradigms for a coupled simulation of carbon and latent heat exchange were tested in comparison with eddy covariance measurements over cropland, grassland and forest ecosystems across the continental U.S. For the purpose of intercomparisons both canopy sub-models were embedded in the Atmosphere-Land Exchange (ALEX) surface energy balance model. While both schemes exploit the linkage between CO₂ assimilation, stomatal conductance and transpiration, the scaled-leaf model incorporates detailed mechanistic descriptions of leaf-level processes and leaf-to-canopy scaling principles whereas the semi-empirical LUE-based model considers the canopy response to its environment in bulk using an analytical expression for stomatal conductance semi-constrained by stand-level measurements of maximum canopy LUE.

Both canopy sub-models were able to reproduce observed magnitudes and variances of carbon and water vapor exchange on hourly and daily timescales with acceptable accuracy considering the simplicity of the ALEX modeling framework and the generality of the applied model parameterizations. Despite the simplicity of the LUE-based model it often performed better than the more detailed scaled-leaf model that has many species-specific tunable model parameters that are a considerable challenge to specify with acceptable accuracy for applications over a variety of vegetative regimes. The use of a deactivation function in the temperature response functions for the Rubisco kinetic properties strongly influenced carbon flux simulations by the scaled-leaf model and resulted in large flux underestimations during early afternoon hours when air temperatures exceeded $\sim 32^\circ\text{C}$. Corresponding simulations by the LUE-based model, that currently does not incorporate effects of extreme temperatures on photosynthetic uptake, were in much better agreement with measurements. These findings suggest that the consideration of species-specific temperature acclimation response functions is critical for a successful implementation of scaled-leaf model parameterizations.

The incorporation of seasonal trends in photosynthetic efficiency (i.e. V_m^{25} and β_n) was needed to avoid bias in model simulations during leaf expansion and senescence at agricultural and deciduous forest sites. The simplistic methodology adopted here scales maximum Rubisco capacity and nominal LUE linearly with green leaf area index and is well suited to application over large regions as green leaf area index can be derived with reasonable accuracy from remote sensing.

Actual light-use efficiencies vary significantly in response to changing environmental conditions and the success of LUE-based modeling frameworks rely on their ability to realistically respond to changes in

light environment, atmospheric humidity, CO₂ concentration and a desiccating environment. The described LUE-based model diagnoses an effective LUE that responds linearly to changes in the ratio of intercellular to ambient CO₂ concentration and the fraction of diffuse radiation, and the incorporation of these important environmental responses into the analytical expression for the stomatal conductance was shown to be critical for tracking diurnal and day-to-day variations in CO₂ assimilation fluxes.

7. ACKNOWLEDGEMENTS

Funding for this research was provided by the National Aeronautics and Space Administration under grant NNG04GK89G. The authors are indebted to the researchers responsible for the micrometeorological and surface flux measurements used in this analysis. Special thanks are given to T.B. Wilson and T.P. Meyers for providing soil surface CO₂ flux data for validation purposes.

8. REFERENCES

- Amthor, J.S., 1989: Respiration and Crop Productivity. Springer-Verlag, New York, 215 p.
- Anderson, M.C., Norman, J.M., Meyers, T.P., Diak, G.R., 2000: An analytical model for estimating canopy transpiration and carbon assimilation fluxes based on canopy light-use efficiency. *Agric. For. Meteorol.*, *101*, 265-289.
- Anderson, M.C., Kustas, W.P., Norman, J.M., 2003: Upscaling and Downscaling – A regional View of the Soil-Plant-Atmosphere Continuum. *Agron. J.*, *95*, 1408-1423.
- Anderson, M.C., Norman, J.M., Mecikalski, J.R., Otkin, J.A., Kustas, W.P., 2007: A climatological study of evapotranspiration and moisture stress across the continental United States based on thermal remote sensing: 1. Model formulation. *J. Geophys. Res.*, *112*, D10117, doi:10.1029/2006JD007506.
- Anderson, M.C., Norman, J.M., Houborg, R., Starks, P.J., Agam, N., Kustas, W.P., 2008: Mapping coupled carbon and water fluxes at the land surface using thermal remote sensing data. *Remote Sens. Environ.* (in press).
- Baldocchi, D., 1993: Assessing the eddy covariance technique for evaluating carbon dioxide exchange rates of ecosystems: past, present and future. *Global Change Biol.*, *9*, 479-492.
- Baldocchi, D., 1994: An analytical solution for coupled leaf photosynthesis and stomatal conductance models. *Tree Physiol.*, *14*, 1069-1079.
- Baldocchi, D., 1997: Measuring and modeling carbon dioxide and water vapour exchange over a temperate broad-leaved forest during the 1995 summer drought. *Plant, Cell Environ.*, *20*, 1108-1122.
- Baldocchi, D., Wilson, K.B., 2001: Modeling CO₂ and water vapor exchange of a temperate broad-leaved forest across hourly to decadal time scales. *Ecol. Model.*, *142*, 155-184.
- Ball, J.T., Woodrow, I.E., Berry, J.A. (1987). A model predicting stomatal conductance and its contribution to the control of photosynthesis under different environmental conditions. In: Biggins, J. (Ed.), *Progress in Photosynthesis Research*. Nijhoff, Dordrecht, pp. 221-225.
- Bernacchi, C.J., Singaas, E.L., Pimentel, C., Portis, A.R., Long, S.P., 2001: Improved temperature response functions for models of Rubisco-limited photosynthesis. *Plant, Cell Environ.*, *24*, 253-259.
- Caemmerer von, S., Farquhar, G.D., 1981: Some relationships between the biochemistry of photosynthesis and the gas exchange of leaves. *Planta*, *153*, 376-387.
- Caemmerer von, S., Evans, J.R., Hudson, G.S., Andrews, T.J., 1994: The kinetics of ribulose-1,5-bisphosphate carboxylase/oxygenase in vivo inferred from measurements of photosynthesis in leaves of transgenic tobacco. *Planta*, *195*, 88-97.
- Campbell, G.S., Norman, J.M., 1998: *An Introduction to Environmental Biophysics*. Springer, New York.
- Campbell, G.S., 1985. *Soil physics with BASIC – Transport Models for Soil-Plant Systems*. Elsevier, New York.
- Chen, D.-X., Coughenour, M.B., Knapp, A.K., Owensby, C.E., 1994: Mathematical simulation of C₄ grass photosynthesis in ambient and elevated CO₂. *Ecol. Model.*, *73*, 63-80.
- Collatz, G.J., Ball, J.T., Grivet, C., & Berry, J.A. (1991). Physiological and environmental regulation of stomatal conductance, photosynthesis and transpiration: a model that includes a laminar boundary layer. *Agric. For. Meteorol.*, *54*, 107-136.
- Collatz, G.J., Ribas-Carbo, J., & Berry, J.A. (1992). Coupled photosynthesis-stomatal conductance model for leaves of C₄ plants. *Aust. J. Plant Physiol.*, *19*, 519-538.
- Crafts-Brandner, S.J., Salvucci, M.E., 2002: Sensitivity of photosynthesis in a C₄ plant, maize, to heat stress. *Plant Physiol.*, *129*, 1773-1780.
- Dai, Y., Dickenson, R.E., Wang, Y.-P., 2004: A two-big-leaf model for canopy temperature, photosynthesis, and stomatal conductance. *Journal Climate*, *17*, 2281-2299.
- De Pury, D.G.G., Farquhar, G.D., 1997: Simple scaling of photosynthesis from leaves to canopies without the errors of big-leaf models. *Plant, Cell Environ.*, *20*, 537-557.
- Dickenson, R.E., Shaikh, M., Bryant, R., Graumlich, L., 1998: Interactive canopies for a climate model. *J. Climate*, *11*, 2823-2836.
- Dreyer, E., Le Roux, X., Montpied, P., Daudet, F.A., Masson, F., 2001: Temperature response of leaf photosynthetic capacity in seedlings from seven temperate tree species. *Tree Physiol.*, *21*, 223-232.

- Edwards, N.T., Hanson, P.J., 1996: Stem respiration in a closed-canopy upland oak forest. *Tree Physiol.*, 16, 433-439.
- Ehleringer, J., Pearcy, R.W., 1983: Variation in quantum yield for CO₂ uptake among C3 and C4 plants. *Plant Physiol.*, 73, 555-559.
- Farquhar, G.D., von Caemmerer, S., & Berry, J. (1980). A biochemical model of photosynthetic CO₂ assimilation in leaves of C3 species. *Planta*, 149, 78-90.
- Gilmanov, T.G., Tieszen, L.L., Wylie, B.K., Flanagan, L.B., Frank, A.B., Haferkamp, M.R., Meyers, T.P., Morgan, J.A., 2005: Integration of CO₂ flux and remotely-sensed data for primary production and ecosystem respiration analysis in the Northern Great Plains: potential for quantitative spatial extrapolation. *Global Ecol. Biogeogr.*, 14, 271-292.
- Gitelson, A.A., Vina, A., Verma, S.B., Rundquist, D.C., Arkebauer, T.J., Keydan, G., Leavitt, B., Ciganda, V., Burba, G.G., Suyker, A.E., 2006: Relationship between gross primary production and chlorophyll content in crops: Implications for the synoptic monitoring of vegetation productivity. *J. Geophys. Res.*, 111, D08S11, doi:10.1029/2005JD006017.
- Goudriaan, J., 1977: Crop micrometeorology: a simulation study. Simulation Monographs, Wageningen.
- Gower, S.T., Kucharik, C.J., Norman, J.M., 1999: Direct and indirect estimation of leaf area index, f_{APAR} and net primary production of terrestrial ecosystems. *Remote Sens. Environ.*, 70, 29-51.
- Gu, L., Baldocchi, D.D., Verma, S.B., Black, T.A., Vesala, T., Falge, E.M., Dowty, P.R., 2002: Advantages of diffuse radiation for terrestrial ecosystem productivity. *J. Geophys. Res.*, 107(D6), DOI 10.1029/2001JD001242.
- Gutschick, V.P., 1996: Physiological control of evapotranspiration by shrubs: scaling measurements from leaf to stand with the aid of comprehensive models. In: Barrow, J.R., McArthur, E.D., Sosebe, R.E., Tausch, R.J. (Eds.), Proc. Shrubland Ecosystem Dynamics in a Changing Environment, Las Cruces, NM.
- Hansen, M., DeFries, R., Townshend, J.R.G., Sohlberg, R., 2000: Global land cover classification at 1km resolution using a decision tree classifier. *Int. J. Remote Sens.* 21, 1331-1365.
- Harley, P.C., Thomas, R.B., Reynolds, J.F., Strain, B.R., 1992: Modelling photosynthesis of cotton grown in elevated CO₂. *Plant, Cell Environ.*, 15, 271-282.
- Houborg, R.M., Soegaard, H., 2004: Regional simulation of ecosystem CO₂ and water vapor exchange for agricultural land using NOAA AVHRR and Terra MODIS satellite data. Application to Zealand, Denmark. *Remote Sens. Environ.*, 93, 150-167.
- Houborg, R., Anderson, M.C., Daughtry, C.T., 2008: Image-based regularization of a canopy reflectance model for automated biophysical parameter estimations. Validation of LAI and leaf chlorophyll for a stressed corn field. *Submitted to Remote Sens. Environ.*
- Jarvis, P.G., 1993: Prospects for bottom-up models. In: Ehleringer, J.R., Field, C.B. (Eds.), Scaling Physiological Processes Leaf to Globe. Academic Press, San Diego, pp. 114-126.
- Kattge, J., Knorr, W., 2007: Temperature acclimation in a biochemical model of photosynthesis: a re-analysis of data from 36 species. *Plant, Cell Environ.*, 30, 1176-1190.
- Kellomaki, S., Wang, K.-Y., 2000: Short-term environmental controls on carbon dioxide flux in a boreal coniferous forest: model computation compared with measurements by eddy covariance. *Ecol. Model.*, 128, 63-88.
- Kim, J., Verma, S.B., 1990: Carbon dioxide exchange in a temperate grassland ecosystem. *Boundary-Layer Meteorol.*, 52, 135-149.
- Kosugi, Y., Shibata, S., Kobashi, S., 2003: Parameterization of the CO₂ and H₂O gas exchange of several temperate deciduous broad-leaved trees at the leaf scale considering seasonal changes. *Plant, Cell Environ.*, 26, 285-301.
- Kubien, D.S., Sage, R.F., 2004: Low-temperature photosynthetic performance of a C4 grass and a co-occurring C3 grass native to high latitudes. *Plant, Cell Environ.*, 27, 907-916.
- Kucharik, C.J., Norman, J.M., Gower, S.T., 1999: Characterization of radiation regimes in nonrandom forest canopies: theory, measurements, and a simplified modeling approach. *Tree Physiol.*, 19, 695-706.
- Law, B.E., Waring, R.H., Anthoni, P.M., Aber, J., 2000: Measurements of gross and net ecosystem productivity and water vapour exchange of a Pinus ponderosa ecosystem, and an evaluation of two generalized models. *Global Change Biol.*, 6, 155-168.
- Lawrence, D.M., Slater, A.G., 2008: Incorporating organic soil into a global climate model. *Clim. Dyn.*, 30, 145-160.
- Leuning, R., 1990: Modelling stomatal behaviour and photosynthesis of Eucalyptus grandis. *Aust. J. Plant Physiol.*, 17, 159-175.
- Leuning, R., Kelliher, F.M., De Pury, D.G.G., Schulze, E.-D., 1995: Leaf nitrogen, photosynthesis, conductance and transpiration: scaling from leaves to canopies. *Plant, Cell Environ.*, 18, 1183-1200.
- Leuning, R., Dunin, F.X., Wang, Y.-P., 1998: A two-leaf model for canopy conductance, photosynthesis and partitioning of available energy. II. Comparison with measurements. *Agric. For. Meteorol.*, 91, 113-125.
- Leuning, R., 2002: Temperature dependence of two parameters in a photosynthesis model. *Plant, Cell Environ.*, 25, 1205-1210.

- Massad, R.-S., Tuzet, A., Bethenod, O., 2007: The effect of temperature on C4-type leaf photosynthesis parameters. *Plant, Cell Environ.*, doi: 10.1111/j.1365-3040.2007.01691.x.
- Massman, W., 1997: An analytical one-dimensional model of momentum transfer by vegetation of arbitrary structure. *Bound.-Layer Meteor.*, 83, 407–421.
- Mayocchi, C.L., Bristow, K.L., 1995: Soil surface heat flux: some general questions and comments on measurements. *Agric. For. Meteorol.*, 75, 43-50.
- Medlyn, B.E., Dreyer, E., Ellsworth, D., Forstreuter, M., Harley, P.C., Kirschbaum, M.U.F., Roux, X.L.E., Montpied, P., Strassmeyer, J., Walcroft, A., Wang, K., Loustau, D., 2002: Temperature response of parameters of a biochemically based model of photosynthesis. II. A review of experimental data. *Plant, Cell Environ.*, 25, 1167-1179.
- Moncrieff, J.B., Mahli, Y., Leuning, R., 1996: The propagation of errors in long term measurements of land atmosphere fluxes of carbon and water. *Global Change Biol.*, 2, 231-240.
- Nijs, I., Behaeghe, T., Impens, I., 1995: Leaf nitrogen content as a predictor of photosynthetic capacity in ambient and global change conditions. *J. Biogeogr.*, 22, 177-183.
- Norman, J.M., 1979: Modeling the complete crop canopy. In: B.J. Barfield and J.F. Gerber (Ed.), *Modification of the aerial environment of plants*. ASAE, St. Joseph, MI.
- Norman, J.M., Arkebauer, T.J., 1991: Predicting canopy light-use efficiency from leaf characteristics. *Modeling Plant and Soil Systems, Agronomy Monograph, No. 31*. ASA-CSSA-SSSA, Madison, pp. 125-143.
- Norman, J.M., Garcia, R., Verma, S.B., 1992: Soil surface CO₂ fluxes and the carbon budget of a grassland. *J. Geophys. Res.*, 97, 18,845-18,853.
- Runyon, J., Waring, R.H., Goward, S.N., Welles, J.M., 1994: Environmental limits on net primary production and light-use efficiency across the Oregon transect. *Ecol. Applications*, 4, 226-237.
- Ruimy, A., Saugier, B., 1994: Methodology for the estimation of terrestrial net primary production from remotely sensed data. *J. Geophys. Res.*, 99, 5263-5283.
- Ryan, M.G., Gower, S.T., Hubbard, R.M., Waring, R.H., Gholz, H.L., Cropper, W.P., Running, S.W., 1995: Woody tissue maintenance respiration of four conifers in contrasting climates. *Oecologia*, 101, 133–140.
- Sellers, P.J., Randall, D.A., Collatz, G.J., Berry, J.A., Field, C.B., Dazlich, D.A., Zhang, C., Collelo, G.D., Bounoua, L., 1996: A Revised Land Surface Parameterization (SIB2) for Atmospheric GCMs. Part I: Model Formulation. *J. Climate*, 9, 676-705.
- Turner, D.P., Urbanski, S., Bremer, D., Wofsy, S.C., Meyers, T., Gower, S.T., Gregory, M., 2003: A cross-biome comparison of daily light use efficiency for gross primary production. *Global Change Biol.*, 9, 383-395.
- Twine, T.E., Kustas, W.P., Norman, J.M., Cook, D.R., Houser, P.R., Meyers, T.P., Prueger, J.H., Starks, P.J., Wesely, M.L., 2000: Correcting eddy-covariance flux underestimates over a grassland. *Agric. For. Meteorol.*, 103, 279-300.
- Wagai, R., Brye, K.R., Gower, S.T., Norman, J.M., Bundy, L.G., 1998: Land use and environmental factors influencing soil surface CO₂ flux and microbial biomass in natural and managed ecosystems in southern Wisconsin. *Soil Biol. Biochem.*, 30, 1501-1509.
- Wang, Y.-P., Leuning, R., 1998: A two-leaf model for canopy conductance, photosynthesis and partitioning of available energy: I. Model description and comparison with a multi-layered model. *Agric. For. Meteorol.*, 91, 89-111.
- Wilson, K.B., Baldocchi, D.D., Hanson, P.J., 2000: Spatial and seasonal variability of photosynthetic parameters and their relationship to leaf nitrogen in a deciduous forest. *Tree Physiol.*, 20, 565-578.
- Wilson, T.B., Meyers, T.P., 2007: Determining vegetation indices from solar and photosynthetically active radiation fluxes. *Agric. For. Meteorol.*, 144, 160-179.
- Wofsy, S.C., Goulden, M.L., Munger, J.W., Fan, S.M., Bakwin, P.S., Daube, B.C., Bassow, S.L., Bazzaz, F.A., 1993: Net exchange of CO₂ in a mid-latitude forest. *Science*, 260, 1314-1317.
- Wohlfahrt, G., Bahn, M., Haubner, E., Horak, I., Michaeler, W., Rottmar, K., Tappeiner, U., Cernusca, A., 1999: Inter-specific variation of the biochemical limitation to photosynthesis and related leaf traits of 30 species from mountain grassland ecosystems under different land use. *Plant, Cell Environ.*, 22, 1281-1296.
- Wong, S.C., Cowan, I.R., Farquhar, G.D., 1979: Stomatal conductance correlates with photosynthetic capacity. *Nature*, 282, 424-426.
- Wullschlegel, S.D., 1993: Biochemical limitations to carbon assimilation in C₃ plants – A retrospective analysis of the A/C_i curves from 109 species. *J. Experiment. Bot.*, 44, 907-920.
- Zhan, X., Kustas, W.P., 2001: A coupled model of land surface CO₂ and energy fluxes using remote sensing data. *Agric. For. Meteorol.*, 107, 131-152.
- Xu, L., Baldocchi, D.D., 2003: Seasonal trends in photosynthetic parameters and stomatal conductance of blue oak (*Quercus douglasii*) under prolonged summer drought and high temperature. *Tree Physiol.*, 23, 865-877.

Table 1A Photosynthesis and stomatal conductance equations of the scaled-leaf canopy sub-model

Equation	Definition	
<i>Photosynthesis and stomatal conductance equations for sunlit (x=1) and shaded (x=2) canopy fractions</i>		
$A_{c,x} = \min\{A_{j,x}, A_{v,x}, A_{s,x}\} - R_{d,x}$	Net rate of CO ₂ assimilation for sunlit and shaded canopy fractions	A1
$A_{v,x} = \begin{cases} V_{m,x} \left(\frac{C_{i,x} - \Gamma^*}{C_{i,x} + K_c(1 + O/K_o)} \right) & \text{for } C_3 \\ V_{m,x} & \text{for } C_4 \end{cases}$	Rubisco limited rate of CO ₂ assimilation for sunlit and shaded canopy fractions	A2
$A_{j,x} = \begin{cases} J_x \left(\frac{C_{i,x} - \Gamma^*}{4(C_{i,x} + 2\Gamma^*)} \right) & \text{for } C_3 \\ \alpha_4 A PAR_x & \text{for } C_4 \end{cases}$	Light limited rate of CO ₂ assimilation for sunlit and shaded canopy fractions	A3
$J_x = \frac{\alpha_3 A PAR_x + J_{m,x} - \sqrt{(\alpha_3 A PAR_x + J_{m,x})^2 - 4\theta_j \alpha_3 A PAR_x J_{m,x}}}{2\theta_j}$	Irradiance dependence of electron transport for sunlit and shaded canopy fraction	A4
$A_{s,x} = \begin{cases} 0.5V_{m,x} & \text{for } C_3 \\ k_T C_{i,x} / (10P) & \text{for } C_4 \end{cases}$	Carbon compound export limited (C ₃), or CO ₂ limited (C ₄) rate of photosynthesis for sunlit and shaded canopy fractions	A5
$\left. \begin{aligned} \theta_3 M^2 - M(A_{j,x} + A_{v,x}) + A_{j,x} A_{v,x} &= 0 \\ \beta_3 A^2 - A(M + A_{s,x}) + M A_{s,x} &= 0 \end{aligned} \right\} \text{for } C_3$	Gross rate of CO ₂ assimilation (<i>A</i>) is solved from nested quadratics to allow for colimitation between <i>A_j</i> , <i>A_v</i> and <i>A_s</i>	A6
$\left. \begin{aligned} \theta_4 M^2 - M(A_{j,x} + A_{v,x}) + A_{j,x} A_{v,x} &= 0 \\ \beta_4 A^2 - A(M + A_{s,x}) + M A_{s,x} &= 0 \end{aligned} \right\} \text{for } C_4$		
$C_{i,x} = C_{b,x} - 1.6R_{c,x}A_{c,x}$	Partial pressure of CO ₂ in the intercellular spaces [$\mu\text{mol CO}_2 \text{ mol}^{-1} \text{ air}$]. The multiplier (1.6) is the ratio of diffusivities of CO ₂ and water in air.	A7
$C_{b,x} = C_a - 1.37R_{b,x}A_{c,x}$	Partial pressure of CO ₂ in the leaf boundary layer [$\mu\text{mol CO}_2 \text{ mol}^{-1} \text{ air}$]. The multiplier (1.37) is the ratio of diffusivities of CO ₂ and water vapor in the leaf boundary layer.	A8
$\frac{1}{R_{c,x}} = b_{c,x} + m \frac{faw \times A_{c,x} RH_{b,x}}{C_{b,x}}$	Stomatal resistance of sunlit and shaded canopy fractions [$\text{mol m}^{-2} \text{ s}^{-1}$]	A9
$\rho_{vb} = \frac{R_{b,x} LE_{c,x}}{\lambda} + \rho_{vac}, \quad e_{b,x} = \rho_{vb} T_{K,x} \Re$	Relative humidity inside the leaf boundary layer for sunlit and shaded canopy fractions.	A10
$RH_{b,x} = 1 - \frac{e^*(T_{K,x}) - e_{b,x}}{e^*(T_{K,x})}$		
<i>Latent heat fluxes</i>		
$LE_{c,x} = \frac{\lambda [e^*(T_{K,x}) - e_{ac}]}{P(R_{c,x} + R_{b,x})}$	Latent heat flux for sunlit and shaded canopy fractions [W m^{-2}]	A11
<i>Temperature response functions</i>		
$k_T = k \cdot 2^{\frac{(T_{K,x} - 298)}{10}}$	Temperature dependence of the initial slope of photosynthetic CO ₂ response (<i>k</i>)	A12
$f(T_k) = k_{25} \exp\left[\frac{H_a(T_{k,x} - 298)}{298\Re T_{k,x}}\right]$	Temperature dependences of <i>K_c</i> , <i>K_o</i> , Γ^* and <i>R_d</i>	A13
$k_{25} = \{K_c^{25}, K_o^{25}, \Gamma^{*25}, R_{d,i}^{25}\}, H_a = \{H_{a1}, H_{a2}, H_{a3}, H_{a6}\}$		
$f(T_K) = k_{25} \exp\left[\frac{H_a(T_{K,x} - 298)}{298\Re T_{K,x}}\right] \frac{1 + \exp\left(\frac{298\Delta S - H_d}{298\Re}\right)}{1 + \exp\left(\frac{T_K \Delta S - H_d}{T_{K,x} \Re}\right)}$	Temperature dependences of <i>V_m</i> and <i>J_m</i> that account for the drop in activity at extreme temperatures	A14
$k_{25} = \{V_{m,i}^{25}, J_{m,i}^{25}\}, H_a = \{H_{a5}, H_{a6}\}, \Delta S = \{\Delta S_v, \Delta S_j\}$		
<i>Leaf to canopy scaling functions</i>		

$V_{m,1}^{25} = V_m^{25} L \left[\frac{1 - \exp(-k_n - k_b L \Omega)}{k_n + k_b L} \right] f_g f_{dry}$	Photosynthetic Rubisco capacity and respiration (at 25°C) of the sunlit canopy fraction	A14
$R_{d,1}^{25} = \frac{R_d^{25}}{V_m^{25}} V_{m,1}^{25}$		
$V_{m,2}^{25} = V_m^{25} L \left[\frac{1 - \exp(-k_n)}{k_n} - \frac{1 - \exp(-k_n - k_b L \Omega)}{k_n + k_b L} \right] f_g f_{dry}$	Photosynthetic Rubisco capacity and respiration (at 25°C) of the shaded canopy fraction	A15
$R_{d,2}^{25} = \frac{R_d^{25}}{V_m^{25}} V_{m,2}^{25}$		
$J_{m,1}^{25} = J_m^{25} L \left[\frac{1 - \exp(-k_d - k_b L \Omega)}{k_d + k_b L} \right] f_g f_{dry}$	Potential rate of electron transport (at 25°C) of the sunlit canopy fraction	A16
$J_{m,2}^{25} = J_m^{25} L \left[\frac{1 - \exp(-k_d)}{k_d} - \frac{1 - \exp(-k_d - k_b L \Omega)}{k_d + k_b L} \right] f_g f_{dry}$	Potential rate of electron transport (at 25°C) of the shaded canopy fraction	A17
$b_{c,1} = b \left[\frac{1 - \exp(-k_b L \Omega)}{k_b} \right] f_g f_{dry}$	The Ball & Berry offset for sunlit and shaded canopy fractions	A18
$b_{c,2} = b \left[L - \frac{1 - \exp(-k_b L \Omega)}{k_b} \right] f_g f_{dry}$		

where

x	=	$x=1$ for sunlit and $x=2$ for shaded canopy fraction
A	=	Absorbed photosynthetically active radiation [$\mu\text{mol m}^{-2} \text{s}^{-1}$]
P	=	Atmospheric pressure at surface [Pa] [$0.1 * \mu\text{mol mol}^{-1}$]
e_a	=	Actual vapor pressure in the canopy air space [Pa]
e_h	=	Actual vapor pressure in the leaf boundary layer [Pa]
e^*	=	Saturation vapor pressure at leaf temperature [Pa]
fa	=	Fraction of available water in the root zone
f_g	=	Fraction of green vegetation
f_{dv}	=	Dry vegetation fraction
k_b	=	Extinction coefficient for direct-beam PAR
k_d	=	Extinction coefficient for diffuse PAR
R_h	=	Leaf boundary layer resistance for water vapor [s m^{-1}]
R_s	=	Stomatal resistance for water vapor [m s^{-1}]
T_k	=	Leaf temperature [$^{\circ}\text{K}$]
ρ_v	=	Absolute humidity in the leaf boundary layer [Kg m^{-3}]
ρ_v	=	Absolute humidity in the canopy air space [Kg m^{-3}]
R	=	Universal gas constant for water vapor [$\text{m}^2 \text{s}^{-1} \text{K}^{-1}$]
λ	=	Latent heat of evaporation [J Kg^{-1}]

Table B1 CO₂ assimilation and stomatal conductance equations of the LUE-based canopy sub-model

Equation	Definition	
$LE_c = \frac{\lambda[e^*(T_K) - e_{ac}]}{P(R_c + R_b)}$	Canopy latent heat flux [W m ⁻²]	B1
$LE_c = \lambda \frac{e^*(T_K)[1 - RH_b]}{PR_c}$	Canopy latent heat flux [W m ⁻²]	B2
$A_c = \frac{C_i - C_a}{1.6R_c + 1.37R_b + R_a} = \frac{C_a - C_b}{1.37R_b + R_a}$	Canopy CO ₂ assimilation (respiration not considered here but it is in Eq. B4!)	B3
$\frac{1}{R_c} = b_c + m \frac{f_{aw} \times A_c \times RH_b}{C_b}$	Bulk canopy stomatal resistance [mol m ⁻² s ⁻¹]	B4
$b_c = b f_{dry} f_g L$		
$A_c = \beta(\gamma) APAR$	Canopy CO ₂ assimilation [μmol m ⁻² s ⁻¹] as a function of LUE and APAR	B5
$\gamma = C_i / C_a$	Ratio of intercellular to ambient CO ₂ concentration (variable)	B6
$\beta(\gamma) = \frac{\beta_n}{\gamma_n - \gamma_0} (\gamma - \gamma_0)$	Linear function modifying LUE in response to modeled C _i /C _a	B7
$\beta_n^* = \begin{cases} \beta_n [1 + 2 \cdot 0.4 (f_{dif} - 0.5)] & \text{for } C_3 \\ \beta_n [1 + 2 \cdot 0.15 (f_{dif} - 0.5)] & \text{for } C_4 \end{cases}$	The effect of the fraction of diffuse lighting (<i>f_{dif}</i>) on the nominal LUE value	B8

where

T_k, R_c, R_b, C_i, C_b, RH_b, b_c represent bulk canopy values. See Table A1 and Table 2 for a description of parameters